An-Najah National University

Faculty of Graduate Studies

EXPERIMENTAL AND MODELING APPROACHES TO STUDY THE EFFECT OF IRRADIATION ON CELL POPULATIONS

By

Khulood Jararah

Supervisors

Dr. Ahmed Bassalat

Dr. Samer Abdallah

This Thesis is Submitted in Partial Fulfillment of the Requirements for the Degree of Master of Physics, Faculty of Graduate Studies, An-Najah National University, Nablus - Palestine.

2023

EXPERIMENTAL AND MODELING APPROACHES TO STUDY THE EFFECT OF IRRADIATION ON CELL POPULATIONS

By

Khulood Jararah

This Thesis was Defended Successfully on 30/10/2023 and approved by

Dr. Ahmed Bassalat Supervisor	Signature
Dr. Samer Abdallah Co-Supervisor	Signature
Prof. Mathilde Badoual External Examiner	Signature
Dr. Ashraf Sawafta Internal Examiner	Signature

Dedication

إلى أعظم المحاربين الذين يخوضون معركة كل يوم مع مرض السرطان و هم مسلحون بالثقة بالله و الأمل و قوة الإرادة.

Acknowledgements

First and foremost, I am very thankful to Almighty ALLAH, the most merciful and the most gracious, for providing me the ability, strength, knowledge, and opportunity to undertake this study and complete it satisfactorily. Secondly, I want to express my most enormous thanks to all people who made the opportunity for this thesis to be completed with their support and encouragement.

The warmest thanks go to my supervisor Dr. Ahmed Bassalat for his invaluable role. His support and assistance not only throughout the thesis but for the whole master's journey have made this journey to be an inspiring experience for me. My co-supervisor Dr. Samer Abdallah many thanks to you for your powerful rule in discussing the experiments and for your brilliant comments and suggestions through all the stages of writing my thesis.

I want to express my gratitude to my supervisors at IJCLab. Prof. Mathilde Badoul and Prof. Olivier Seksek. Thanks for always positively guiding me and making me feel confident in my abilities. The conversations and meetings inspired me to think outside the box. I would also like to thank my friend Marianne Billoir who made enjoyable moments during my work.

I am also grateful to all the committees of the Winter School in High Energy Physics in Palestine (WISHEPP). Prof.Achillie Stocchi, Dr.Hadil Abualrob, and Prof.Philippe Laniece, you just gave me a chance to have a unique scientific and human experience.

My greatest thanks go to my backbone: my dad Dahi, my mom Itemad, my lovely husband Mohammed and to my heroes, my siblings: Fawz, Wesam, Salam, Majd, Musab, Abd-alrahamn, Ayman, Ahmed and Bashar. Thanks for your prayers and the unconditional love you gave to me. Thanks to my family in law, you have always shown me your support during my work.

Many thanks to my best friends: Afnan, Hala, Ahlam, Amani, Eman, and Dana you have always been the light of my life. I am also grateful to my support team in exile: Theraa, Masa, Rasha, Manar, Shyma’a, and Reema. I really appreciated all of your encouragement.

Declaration

I, the undersigned, declare that I submitted the thesis entitled:

EXPERIMENTAL AND MODELING APPROACHES TO STUDY THE EFFECT OF IRRADIATION ON CELL POPULATIONS

I declare that the work provided in this thesis, unless otherwise referenced, is the researcher's own work, and has not been submitted elsewhere for any other degree or qualification.

Student's Name: Khulood Dah: Naeem Jararah

Signature: 

Date: 30/10/2023

Table of Contents

List of Tables

List of Figures

List of Schemes

List of Appendices

Experimental and Modeling Approaches to Study the Effect of Irradiation on Cell Populations

By
Khulood Jararah
Supervisors
Dr. Ahmed Bassalat
Dr. Samer Abdallah

Abstract

In recent years, exceptional development is made towards a better understanding of proposed hallmarks of cancer treatment. However, with its high incidence, in the 21st century, it is still a challenge to find the optimum technique to treat cancer. Despite the different treatment modalities such as surgery, chemotherapy, radiation therapy, immunotherapy, and hormonal therapy, radiation therapy remains an essential component of tumor treatment; the main goal of tumor radiotherapy is to control and inhibit the proliferation of a malignant tumor cell. Even though a well-known feature of cancer cells promotes processes such as aggressiveness, metastasis, and invasiveness that have been associated with a worse clinical prognosis, this feature is the acidosis of the tumor microenvironment. Acidification of the tumor microenvironment comes due to the high glycolytic activity in cancer cells leading to extensive lactate production. Depending on the knowledge of cancer biology and radiation physics, the principles, methodologies, and techniques used to study the effect of ionizing radiations and the pH (intra and extracellular) on the cell growth of the F98 glioma cell line are discussed in this context.

The first part of the thesis was the experimental part. The first section of the experimental part was to study the extracellular pH (pHe) as a therapeutic target to optimize the efficacy of radiotherapy, as this section focused on studying the cell growth and cell viability after placing the cell under different pH solutions and using different doses of radiation, the results in this part have hypothesized that changing the pHe will result in predictable changes in the radiation efficiency, which gives an argument for considering pH as a therapeutic target for future research based on the summation of radiotherapy with pH-regulating agents.

The second section measured the intracellular pH (pHi) of the glioma F98-cell line. The results of this experiment gives an argument for considering the changes in pHi due to the

radiation as a new biological effect of radiation on the cancer cell, these results were very interesting, but still, they need to be approved.

The second part of the study was computational modeling or simulation, where in this work, a model was built to describe the cell growth of our cell line. The simulation results were able to give the same experimental data trend. Regardless the fact that the simulation can be developed to add more variables to give more information about the system.

Keywords: Glioma; Proliferation; pH; Radiation; Radiotherapy.

Chapter One
Introduction

This thesis is considered a specialty of the biomedical physics field that is concerned mainly with the medical application of radiation and combining it with cell biology to develop a treatment of solid tumors in general and the brain tumors in particular.

Tumor Radiotherapy is a technique used to control the proliferation and inhibit a malignant tumor cell using different types of ionizing radiation. Traditionally, radiation can directly affect the structure of the DNA and induce other therapeutic effects against the regular mitosis events of the tumor cells (1) . The latest studies have shown that radiation can change the tumor cell microenvironment and alter the biological behavior of cancer cells.

From the biological point of view, cancer cells can acidify their environment due to their high glycolytic activity. In contrast, they can maintain their intracellular pH to be normal or Alkaline (2); this helps the tumor to proliferate and to be more aggressive and creates a perfect storm for metastatic progression (3). Some research has demonstrated that lowering intracellular pH minimizes the cancer cell's proliferation rate (4). This thesis aims to focus on the combined effect of the pH (intra and extracellular) and ionizing radiations on the cell growth.

The outcomes of studying the effect of radiation on cell populations will help in future clinical and biological research by predicting the efficiency of radiation therapy and estimating the health risks of exposure to this radiation. Also, to highlight how the obtained results will guide the development of new treatment techniques, emerging therapeutic strategies towards more effective tumor therapy.

This chapter gives a general overview of radiation, representing its definition, types, and sources. Moreover, it concerns the interaction that occurs between radiation and matter, as it is one of the concepts that will help later in understanding the effect of radiation on biological systems.

1.1 Physics Background

1.1.1 Radiation

Radiation is the emission of energy as electromagnetic waves or subatomic particles by a source. And this emission could happen naturally or artificially. Regardless of the radiation source, radiation exists all around us such as cosmic rays, and it can be classified into two forms according to its energy: Ionizing radiation and Non-ionizing radiation. The word ionizing comes from ionization, which means producing ions by removing electrons from the molecules or atoms of the materials or medium through which the radiation passes. First, non-ionizing radiation, such as Microwaves and Radio waves, this type of radiation does not have that much energy to produce ions in the medium. Non-ionizing radiation is not a serious health risk. However, when it passes a medium, it causes atoms to vibrate, which can cause them to get hotter.

Ionizing radiation has a unique capability to cause ionization (producing ions) in the medium through which it passes. This type of radiation can penetrate the human body, and it is strong enough to directly damage the DNA or affect the structure of molecules, causing cell killing and stopping the cells from growing. Ionizing radiation originating from nature is typically at low levels; this means we are exposed to a small amount of ionizing radiation daily.

There are two types of ionizing radiation depending to its type:

- Photon radiation: x-rays and gamma rays.
- Particle radiation: such as electrons, protons, neutrons, alpha particles, and beta particles.

Despite the health risks that may be caused by ionizing radiation, an optimal quantity of ionizing radiation can be used for both therapeutic and diagnostic purposes. This kind of radiation has become a standard of care for treating many types of cancer.
Ionizing radiation falls into two families according to its source: natural and man-made (Artificial).

1.1.2 Sources of Ionizing Radiation

1- Natural radiation

Natural radiation happens because of the existence of radioactive materials. These types of elements, for some reason, are unstable, so they emit radiation spontaneously when they undergo radioactive decay in order to shift to a more stable atom. The radioactive reactions happen because in different areas of the Chart of the Nuclides Fig.(A.1) (5), one or the other will shift the product as close as possible to the region of stability where the optimal value of the proton-neutron ratio is around 1:1 for small nuclei ($Z < 20$), and at high Z the ratio decreases slowly to about 0.632 (6). These interactions should obey conservation laws such as conservation of charge, mass number, mass and energy, and conservation of momentum.

As follows is a brief explanation of the different types of radioactive decays that the unstable atoms may take to bring them to a more stable configuration:

1- Alpha decay (α- decay)

This type of radioactive decay occurs most often when a nucleus's proton-neutron ratio (Z\N ratio) is too high. In this process, these heavy nuclei eject a positively alpha particle that consists of two protons and two neutrons (is the nucleus of a Helium atom); this implies reducing the Z\N ratio in the parent nucleus. The emission of an α particle brings a daughter nucleus with an atomic number less than 2 and a mass number less by 4, concerning the parent nucleus

$$^{A}_{Z}X \longrightarrow {}^{A-4}_{Z-2}X' + {}^{4}_{2}He^{2+} \qquad (1.1)$$

α particles have a mass approximately equivalent to 4 protons, so they are relatively heavy and slow in contrast to other types of nuclear radiation. Also, these particles are strongly ionizing because they are highly charged; they cannot penetrate very deep through the medium. They are stopped by a few centimeters of air or less than a tenth of a millimeter of biological tissue.

2- Beta decay (β-decay)

There are two types of beta decay:

a-β^--decay

A type of radioactive decay in which a negatively charged beta particle (A high-speed negative electron) is emitted from a rich neutrons unstable atomic nuclei so it has the ratio of Z/N in the nucleus is too low in order to get the parent nucleus as close as possible to the optimal Z\N ratio. At the nuclear level, this occurs when a neutron in the unstable nucleus is transformed to yield a proton, increasing the atom's atomic number. To be more specific, as known, the proton and neutron consist of elementary particles called quarks. So, a down quark inside the neutron converts into an up quark via a weak nuclear force, varying the neutron into a proton. The proton has a positive charge, but the neutron is neutral. So in order to obey the conservation of charge law, the nucleus generates a negative electron (β particle) and an antineutrino.

$$^{A}_{Z}X \longrightarrow {}^{A}_{Z+1}X' + \beta^- + \bar{\nu}_e \qquad (1.2)$$

β^- particles are equivalent to electrons in mass and charge, and they have much less ionizing potential than α particles, so they have higher penetrating power than α particles, so they are brought to rest by about 1 cm of soft tissue. They can penetrate 4 m of air.

b- β^+-decay

Similarly to β^--decay, β^+-decay occurs in unstable nuclei that have many protons. Hence, it has a high Z\N ratio, so to bring the Z\N ratio closer to its optimum value, the proton is converted to a neutron. More clearly, an up quark inside the proton converts into a down quark, changing the proton into a neutron. This yield a decrease in the atom's atomic number.

$$^{A}_{Z}X \longrightarrow {}^{A}_{Z-1}X' + \beta^+ + \nu_e \qquad (1.3)$$

β^+ particles are the same as the positron (electrons with a positive charge)

3- Gamma decay (γ- decay)

Unlike alpha and beta decay, no particles are emitted from the atomic nuclei in this form of the radioactive decay process. Instead, high-energy electromagnetic radiation is released (a gamma ray photon). Here the nucleus is excited and has extra energy to be stable. During this type of decay, the number of protons stays unchanged.

$$^{A}_{Z}X^{*} \longrightarrow {}^{A}_{Z}X + \gamma \qquad (1.4)$$

Even gamma rays have the least ionizing power; they can penetrate materials more intensely than the charged particles ejected during alpha and beta decay. Gamma rays can be stopped by a few centimeters of lead. Unsurprisingly, they can penetrate deep inside the body and cause damage to the cells.

4- Electron Capture

During electron capture, a proton-rich unstable nucleus absorbs an electron in an atom's inner shell, commonly from the L or K electron shells, where it couples with a proton, producing a neutron and a neutrino. So the neutrino is released from the atom's nucleus since an atom loses a proton during this process, which decreases the atom's atomic number. Following the capture of the inner electron, an electron from the outer shell returns the electron that was captured and influences the emission of characteristic X-ray photons.

$$^{A}_{Z}X + e^{-} \longrightarrow {}^{A}_{Z-1}X' + \nu_{e} \qquad (1.5)$$

These are only some of the ways to natural radiation. There are other natural sources of radiation, such as radiation from space (cosmic and solar radiation) and radiation from Earth.

2- Man-made radiation

Due to the importance of radiation, people have been sought to design methods to produce these rays and to use them in several areas of scientific and practical life. So, we have heard about particle accelerators being a common artificial way to produce radiation which will be discussed in the next section.

Particle Accelerators

Particle accelerators are machines used to accelerate beams of charged particles. Accelerator science is not only for fundamental research that is used for an improved understanding of matter. It also has a powerful role in topics related to Medicine, Detectors, Nanoscience, and Nuclear research.

Particle accelerators could be linear accelerators or circular accelerators. The main difference between the basic types of particle accelerators is that linear accelerators can be used for fixed-target experiments. In contrast, the circular accelerator is used for both fixed-target experiments and colliding beams. These accelerators have different sizes. They could be tens of kilometers or fits in small rooms that depend on their rule or use, but all accelerators have these main components, as it shows fig. (A.2):

1- The particle source: The particle source provides charged particles to be accelerated, such as electrons or protons.
2- A component that accelerates the charged particles, such as an RF power generator. Which, in principle, uses an electric field separated around the accelerator in which, at a given frequency, they change polarity from positive to negative, and creating radio waves that accelerate particles in bunches
3- Drift tube: The beam of the accelerated particles travels inside a vacuum tube to maintain an environment free from dust and air to prevent any dissipation of the beam
4- Magnets steer and focus the beam or change their trajectories while it travels through the drift tube.

With the advancement of accelerator science, new techniques have been developed to treat cancer and diagnose various diseases. So, the medical particle accelerators appeared.

Linear Accelerators (LINACS)

LINAC is a linear accelerator used to deliver high-energy photons for the treatment of

superficial and deep-seated tumors.

LINACS are commonly used to treat tumors with external beam radiation. The first LINAC used for patients' treatment was at Stanford University in the United States in 1956; it was large and bulky with limited gantry rotation. Then, between 1962 and 1982, the LINACs developed to be better in precision and accuracy and also to be isocentric, meaning the gantry could rotate up to 360 degrees. The current lINACs are computer-driven; they have upgraded to accuracy and improved precision, dose rates, field sizes, and operating modes (7).

To generate the beam in a LINAC, the electrons produced by heating a tungsten filament within the cathode; the temperature of the filament controls the number of electrons

injected. After this, they then injected into the waveguide, radio frequency waves are pulsed in the waveguide by an RF power generator (magnetron or klystron); this is synchronized with the injection of electrons into the waveguide by the electron gun. Radiofrequency waves accelerate the electrons along the waveguide to a relativistic speed; this speed is adjusted by controlling the power and the frequency of the radio frequency waves, which are controlled by the magnetron. The waveguide, in its basic form, is an evacuated tube that contains a series of metallic (copper or aluminum) disks with small holes in the center or irises; these irises divide the accelerating waveguide into a series of cylindrical cavities, and the electrons are accelerated through the cavities utilizing an oscillating electric field supplied by the RF generator, a vacuum is created to ensure that other particles do not impede the electron beam. The path of the negatively charged electron beam is controlled by two sets of quadrupole magnets that surround the waveguide. An additional two sets of focusing coils help to define the electron beam further so that it is very fine with a diameter similar to that of a pinhead. The beam exits the waveguide and is then redirected and bent by bending magnets to hit and interact with a target at the opposite end of the accelerating waveguide, creating X-ray (photons) beam paths for different energies.

When the high energy electrons hit the target where the electron energy excites the target, which in turn emits a photon, the high energy photons emerge from the target in a variety of directions, then a primary collimator only allows forward traveling photons to pass through, producing a cone-shaped beam, the primary collimator minimizes leakage and therefore excess total body dose by absorbing scattered photons traveling in the lateral direction and also defines the maximum size of the resulting clinical beam. This beam then is shaped in a way to satisfy the shape of a patient's tumor by a multileaf collimator (MLC) which is a device invented of individual leaves of high atomic number material such as tungsten or lead; they can freely move in and out of a particle beam to suit the shape of the tumor of the patient. Both the Gantry system and the treatment couch rotate in a way to deliver the radiation at different angles around the patient(8), see Fig. (A.3).

1.1.3 Interaction ionizing radiation with matter

Understanding the interactions between ionizing radiation and matter will lead to a good understanding of how this radiation will affect biological systems. As reported before, ionizing radiation is classified depending on its type; also, it can be familiarized

depending on the charge into charged ionizing radiation or direct ionizing radiation such as alpha and beta particles and uncharged (Neutral) ionizing radiation or indirectly ionizing radiation because this type does not form significant ionization such as photons (Gamma rays and X rays) and neutrons. So, the interactions between charged particles with matter and the interactions between photons and matter will be introduced in detail in this section.

Starting with the interaction that occurs between the charged particles with matter, energetically charged particles interact with matter through:

1-coulomb force
2-Or lose their kinetic energy (9) by:

- **Excitation**: Excitation occurs when energy is transferred to an orbital electron causing it to jump to a higher energy orbit; the atom then is excited, and after a short time, the excited electron returns to its original energy level with a mission of electromagnetic radiation.

- **Ionization**: Ionization occurs if the energy of the incident particle exceeds the binding energy of an atomic electron it interacts with. The atomic electron is completely removed from the atomic shell via charged particle interactions, leaving a positive ion and a free electron. The energy of the ejected electron is the incident energy minus the binding energy. Charged particles like electrons and heavy ions like protons and deuteriums cause direct ionization. The important thing is that the ejected electron will also interact with nearby atoms producing secondary ionizations leading to the production of delta rays.

After ionization, an ion pair (IP) is formed, which consists of the ejected electron and positively charged ion, the average energy required for a charged particle to produce an ion pair in the air is called ion pair energy, and it is denoted by W, where W is 33.85 eV/ion pair (10), the ion pair energy includes energy used to overcome electrons binding energy, excitation and interaction with other atoms, and kinetic energy of the ejected electron, the average energy required for a charged particle to produce an ion pair in soft tissue is 22 eV/ion pair. The average number of primary and secondary ion pairs generated per unit length of the charged particle path is defined as specific ionization (SI); it is expressed in ion pairs per millimeter (IP/mm), and SI is proportional to the squared charge

of the incident particle and inversely proportional to the squared incident particle velocity $SI \propto Q^2/v^2$

As the charged particle moves through a medium such as air, it slows down because it loses its energy by ionization and producing more ion pairs, so its specific ionization increases to a peak called the Bragg peak.

This leads to introduce another critical term which is linear energy transfer (LET) and defined as the average amount of energy deposited locally in an absorber per unit path length; it is a description of local energy deposition in a medium and has an impact on absorbed dose to tissues, which also highly determine the biological consequence of exposing to radiation. LET is equal to specific ionization multiplied by the ion pair energy.

$$LET = SI \times W \tag{1.6}$$

LET can also be expressed as the squared charge divided by a particle's kinetic energy

$$LET \propto Q^2/K.E \tag{1.7}$$

Another mark is that the interactions between the heavily charged particles with matter differ from those between the light-charged particles and matter. One way to differentiate between heavy-charged particles and light-charged particles is to observe the ionization path in the matter. Heavy-charged particles like alphas make short, dense straight-line tracks in the matter, while light-charged particles like electrons follow a more scattered, less dense ionization path in the matter. The path length of a particle is defined as the distance the particle travels; light-charged particles like electrons cover longer path lengths or distances than heavy-charged particles. The alpha particles' path and range are equal, while the electron path is longer than its range; alpha particles also deposit more energy over a short range than electrons.

The range of a charged particle (R) is a straight-line distance it travels before coming to a complete stop; R is equal to particle energy (E) divided by LET.

$$R = E/LET \tag{1.8}$$

this formula is applicable to heavy, highly ionizing particles such as alpha particles that travel in a straight line while losing kinetic energy.

- **Radiative losses**: Radiative losses happen due to the deceleration of the charged particles as it interacts with the nucleus. This results in bremsstrahlung radiation which is called bremsstrahlung X-rays. Bremsstrahlung is a German word for breaking energy, so when the electron comes in and approaches the nucleus and hence is attracted by the positively charged nucleus if it has a high velocity, it can keep moving, but its path is curved around, and it is giving up some of its energy, and it is going to slow down a little bit so its energy going to go down. There is a relation between radiative energy losses and ionization energy losses; it is expressed as

Radiation energy loss/ Ionization energy loss $\propto$ KE x Z

This formula is used to select target materials for X-ray production, which means higher atomic number targets are better at X-ray production. These types of materials are efficient as X-ray targets in linear accelerators.

Interaction photons with matter

Neutral radiation cannot directly interact with matter by coulomb forces, but they interact with matter via four interactions. These are classical scattering or Rayleigh scattering, photoelectric absorption, Compton scattering, and pair production. The probability for each process is influenced by many factors, including the photon energy and the properties of the material being traversed. It is highly driven by the absorber atomic number (Z).

Looking at the different interactions that a photon will undergo with matter

1- **Rayleigh scattering**: This process involves the excitation of the total atom; there is no ionization. After Rayleigh scattering, there is no difference in energy between the incident and the scattered photon because the scattering is elastic. This interaction occurs for low-energy photons. This type of scattering happens infrequently in diagnostic imaging

2- **Photoelectric absorption**: This interaction happens when an inner shell electron (usually k-shell electron) absorbs an incident photon with a specific energy, causing the electron to be ejected from the atom. After the ejection of the electron, an outer shell electron will undergo to fill the place of the missing (ejected) electron; in this process, the outer shell electron will lose energy by giving up a characteristic X-ray or/and an Auger Electron

The probability of photoelectric absorption varies directly as the cube of the atomic number of the absorber and inversely as a cube of photon energy. The threshold photon energy required for photoelectric absorption is equal to the electron shell's binding energy, which is called the absorption edge. At the absorption edges, the photoelectric absorption probability greatly increases. This case is called Resonance.

Photoelectric absorption dominates when lower energy photons interact with high atomic number material; it is used to amplify differences like the differential absorption between tissue and contrast materials.

3- **Compton scattering**: In this event, an incident photon interacts inelastically with an nearby free electron, so the photon passes some of its energy to the electron. This causes the ejection of the electron from its orbital. Here the scattered photon has less energy and so a longer wavelength. The probability of Compton scattering is almost independent of the atomic number (Z) but varies linearly with the electron density (number of electrons per unit mass). It predominates in the soft tissues at energies above 100 keV, as it also decreases with the photon energy. It is considered the most probable interaction in the diagnostic energy range between 50 and 150 keV (11).

4- **Pair production**: Pair production occurs via an interaction between a photon and a nucleus. In pair production, a photon is converted to an electron/positron pair; both electron and positron lose their energy by excitation and ionization and come to rest after a short distance. When the positron comes to rest, it interacts with an electron in an annihilation reaction to produce a pair of photons of 0.511 MeV radiation.

This interaction will occur only if the threshold energy of the photon is equal to 1.02 MeV (which is twice the rest mass of an electron)

In pair production, a photon transitions to an electron/positron pair. The presence of a massive particle is required. This allows for energy conservation and momentum as the massive particle can absorb some recoil energy.

Suppose the photon energy is very high and interacts with an atomic nucleus, leading the nucleus to decay into particles such as protons, alpha particles, neutrons, and other massive nuclides. This process is called photodisintegration.

Chapter Two
Radiotherapy and Tumor microenvironment

2.1 Radiation therapy

Radiation therapy (Radiotherapy) is an efficient tool that uses ionizing radiation to kill cancer cells or to relieve their growth by damaging their DNA. Approximately 50% of all patients with localized malignant tumors will benefit from radiation therapy as part of their treatment (12). When radiation damages the genes (DNA) in cells. Genes control how cells grow and divide; they can't grow and divide anymore. Over time, the cells die. Meaning that radiation can be used to kill cancer cells and shrink tumors. However, Radiation therapy does not destroy cancer cells immediately. It takes days or even weeks of treatment before DNA is injured enough for cancer cells to die. After that, cancer cells keep dying for weeks or months after radiation therapy ends. That all depends on the life cycle of a cell.

2.1.1 Radiotherapy techniques

There are two main techniques used in radiation therapy:

1- External Radiotherapy

External radiotherapy means that the radiation source is situated outside the patient. And this technique is classified as a local treatment, meaning it treats a specific body part. External radiotherapy uses radiation usually generated by a linear accelerator (LINAC), which has been discussed in the previous section.

For each patient in this treatment technique, a treatment plan is always managed before the irradiation sessions happen, in addition to the full dose to be given during the planned radiotherapy course. This plan usually defines the target area to be treated, the dose distribution (dosimetry), the fractions used in each session, and the duration of each session.

2- Internal Radiotherapy

The internal beam is a treatment in which the radiation source is plant inside the body. This technique is classified depending on the form of the radiation source into two forms: brachytherapy and systemic therapy.

Brachytherapy utilizes a solid radiation source that is injected inside the area to be treated. This means that brachytherapy is a local treatment that treats only a specific part of the body. The common radionuclides used in brachytherapy are cesium 137 (Cs^{137}), iridium 192 (Ir^{192}), and radium 226 (Ra^{226}). These radionuclides come in the form of sealed sources means that they are permanently sealed in a capsule or bonded and in a solid form such as wires, needles, or tubes. The sources remain in place in the patient for the duration of the treatment time.

The other technique is systemic therapy, which uses a liquid source of a radioactive substance such as iodine. Systemic means the treatment travels in the blood to tissues throughout the body, seeking out and killing cancer cells. The drugs, in this case, can be put into a vein or given by mouth (13, 14).

The type of radiation therapy given to a patient depends on the type of cancer being treated, its size, its location inside the body, and its closeness to radiation-sensitive body tissues, taking into account the patient's age and medical history (15).

2.1.2 Cell and radiation

Determining the effect of ionizing radiation on any biological system starts by studying the impact of this radiation on the cellular level, in other words evaluating how much the cells are sensitive to radiation which is called the radiosensitivity of the cell. Measuring the cellular effect on radiation and the cellular response to radiation depends on some biological factors related to the organism and physical factors related to the type and delivery of the radiation.

Two French scientists called Bergonie and Tribondeau were first described cell radiosensitivity: They postulated a law with their name stating, "The radiosensitivity of a cell is directly proportional to reproductive rate and is inversely proportional to its degree of differentiation."(16) Meaning that radiosensitivity increases in the cells that are rapidly dividing (actively proliferating) and poorly differentiated, i.e., cells that are very simple or they do not have a specific function (low degree of specialization). Also, radiosensitivity increases for the cells with high oxygen levels because oxygen enhances free radical damage, which will be described in detail in the following sections. In addition, the radiosensitivity is dependent on the cell cycle of the cell(17, 18), where the

cell itself will be less or more sensitive depending on the cell stage in the cell cycle. This relation will be discussed shortly in the next section.

2.1.2.1 Cell cycle

Understanding the cell cycle is essential in studying the cell's radiosensitivity, which depends upon the cell phase in the cell cycle.

The cell cycle comprises four phases: The G1 phase, the S phase, the G2 phase, and the M phase. The two most important phases are the S phase and the M phase. During the S phase or the synthesis phase, DNA is replicated. The cell divides into daughter cells from a single parent cell for the M phase or mitosis phase. The G1 and G2 phases refer to Gaps because these phases correspond to intervals between the M and the S phases. The following paragraph briefly explains what happens during each stage in the cell cycle.

Starting with the G1 phase, the cell performs its daily functions, grows, and synthesizes the proteins required for DNA replication; after this, the amount of DNA is replicated in the S phase; in the G2 phase, the cell prepares for mitosis, and additional proteins are synthesized. The final phase is the M phase, in which cell division occurs; the chromatids are separated evenly between two daughter cells.

According to the nature of the cell, there are three options after mitosis: First option, if further cell division is required, the cells re-enter the G1 phase and prepare for the S phase; the second one, if further cell division is not required, but potentially at a later stage, the cell may enter a resting phase, called the G0 phase. Once the cell is in the G0 phase, it can exit and re-enter the G1 phase. This is regulated by external signals, such as growth factors, which bind to receptors and initiate an array of signals that trigger cell division. In most cases, the last option is that the daughter cells make an irreversible exit from the cell cycle and differentiate.

What should be noted is that the process of cell division is prone to errors, and no genetic errors must be passed on to the daughter cells. To deal with such errors, the cell cycle has checkpoints at certain stages; these checkpoints ensure that the requirements for the next phase are fulfilled.

At the end of the G1 phase, the cell is examined for any DNA damage and whether necessary substrates are available for DNA replication. If necessary, the cell cycle is

stopped to repair any damage. In the G2 checkpoint, the cell is examined for incomplete DNA replication. If this is the case, the cell can initiate programmed cell death, also termed apoptosis, to prevent damaged genes from being passed on. The M checkpoints, which occur during mitosis, determine whether the chromosomes are about to be correctly distributed. All of these checkpoints are necessary because errors are frequent, and the checkpoints ensure the integrity of the cell's genome, all of this is summarized in Fig. (A.4).

The cell cycle is internally regulated by proteins called cyclins. They determine whether a cell transitions into the next phase. Cyclin activity is influenced by some proteins.

In cancer cells, the function of cell cycle checkpoints is usually limited; this leads to uncontrolled cycling, even in the presence of DNA damage. Cancer cells are also independent of growth signals and initiate the cell cycle, even though cell division is not required.

So, after talking about the cell cycle, the cells are less radiosensitive in G0, in early G1, and the late S phase of the cell cycle because the cell has two copies of its DNA and contains an amount of repair enzymes. In contrast, they are more radiosensitive in late G1, G2, and throughout the M phase of the cell cycle (19).

2.1.2.2 How does the radiation work on the cancer cells?

Radiation exposure can cause a defect on the cellular level and breaks within the DNA, and these breaks could directly by disrupting biological molecules by hitting the DNA of a cell or indirectly through radiolysis of water, which in turn can generate reactive chemical species that may damage nucleic acids, proteins, and lipids (20).
The indirect way, this action is the most likely pathway since the body mostly contains water. Radiation will interact with water, and when radiation interacts with water, it causes water to radiolysis; lysis means breaking down. The incoming photon which interact with a water molecule, and the last will be ionized, then break apart, forming reactive chemical species called free radicals. Free radicals are atoms or molecules identified by the presence of a single unpaired orbital electron (which means that it has a single unpaired valence electron). They are unstable and highly reactive (very interactive); those free radicals have a lifetime of approximately 10^{-5} seconds. During this time, they interact with everything around them, so they are interacting with other atoms, and hence, they are

creating ionizations and excitations, but it is also creating toxic substances (21). This happens when the water molecule is ionized, producing an ion pair, positively charged water molecule (H_2O^+) and the electron (e^-) that was ejected; since the positively charged water molecule is unstable, it goes to dissociate into a hydrogen ion (H^+) and hydroxyl (OH^-), here the hydroxyl is the free radical.

Now, the electron that is ejected will also combine with an adjacent water molecule resulting in a negatively charged water ion (H_2O^-), again this negative water ion is unstable and will also break apart into a negatively charged hydroxyl (OH^-), and hydrogen (H^+), here the hydrogen is the free radical.
Following the reaction that occurs in the ionization of water:

$$H_2O + \text{X-Ray} \longrightarrow H_2O^+ + e^- \quad (2.1)$$

then

$$H_2O^+ \longrightarrow H+ + OH^-* \quad (2.2)$$

the second reaction

$$H_2O + e^- \longrightarrow H_2O^- \quad (2.3)$$

then

$$H_2O^- \longrightarrow H^+* + OH^- \quad (2.4)$$

* indicates the free radicals.
Here is another illustration of the radiolysis of water. If the hydroxyl free radical joins with another one, this produces peroxide (H_2O_2), and if the hydrogen radical joins with others, it can produce superoxide (O_2^-) radical; these are toxic substances. So free radicals can ionize atoms, excite atoms, and produce these toxic substances, potentially damaging the cells. The two main ones occur when hydroxyl radicals join other hydroxyls producing

peroxide; the other is when hydrogen free radical joins with two oxygens and produces hydroperoxyl free radicals. As shows Fig. (A.5)

This shows an agreement with what was mentioned above that the cells with high oxygen levels would be more radiosensitive because oxygen enhances free radical damage.

This damage occurs less commonly for the direct pathway because radiation interacts randomly with relatively few DNA molecules in the cell. As noted before, most interactions should occur in H_2O since water is the most abundant molecule. In this way, the radiation directly hits the DNA and breaks it.

The damage in the DNA could be repaired when the cell cycle is stopped at the specific checkpoint to repair the damage. The repair process depends on the type of break that happens in the DNA (22). As known, DNA shapes like a double helix and each side of this helix is called a "strand." When the radiation hits a cell, it may cause a single-strand break (SSB). In this case, only a single strand is damaged; this type of break is considered easy to repair. SSBs commonly occur due to indirect DNA damage (23). The other case occurs when both strands are damaged and is called a double-strand break (DSB), the breaks could be at a different spot, and this occurs when each strand is exposed to a single-strand break at a different time; this damage also can be repaired. However, if the breaks happen at the same spot, it will be harder for the cell to repair, leading to cell death because the DNA will be separated into two fragments. The DSB occurs when ionizing radiation (especially alpha radiation) directly hits the DNA. The strand breaks may happen the most when the cell is in its M phase because it is well-oxygenated in this phase.

These effects of radiation are considered for both cancer cells and normal cells; this means that the radiation also causes damage in the normal tissues, which can be considered a side effect of radiotherapy. The next section will talk about the biological side effect of radiation. Also, it will include a technique to reduce this effect as much as possible. But as reported before, the cells are more sensitive to radiation in its M phase, and cancer cells divide more frequently than normal cells. Cancer cells become more vulnerable to radiation as their cell cycles repeat more frequently than normal cells. Luckily normal cells heal better than cancer cells.

2.1.3 The biological side effect of radiotherapy

Despite the advantages of radiotherapy and its role in killing cancer cells by inhibiting or stopping their mitosis and proliferation. Like any other treatment technique, radiotherapy can affect normal tissues and causes harmful injuries to normal cell.

When cancer cells are irradiated, some nearby healthy cells are also irradiated. The effects of radiation will be considered for both cancer cells and normal cells, and this causes injury to both of them. However, the cells are more sensitive to radiation in their M phase, and cancer cells divide more often than normal cells. Cancer cells become more vulnerable to radiation as their cell cycles repeat more frequently than normal cells. Luckily normal cells heal better than cancer cells.

A tumor will contain thousands of cancer cells, so if a one-time giant dose of radiation is delivered, not every cell would be in its M phase and, therefore, not equally affected. In order to distribute damage, the total dose of radiation should be broken up into smaller amounts even over multiple days, this is called fractionation. This increases the chance of radiation catching a cell in its M phase and causing adequate DNA damage. On the other hand, this method can minimize damage to healthy tissues because splitting the radiation dose permits healthy cells to repair and fix this sublethal damage between the fractions where normal cells are more capable of repairing the damage to their DNA than cancer cells (24).

Nevertheless, some research has discovered that a new phenomenon can cause damage to normal cells even though they have not been irradiated directly, and it is called the bystander effect. So, the affected cell warns other cells by releasing some molecules, such as cytotoxic molecules, to warn its neighboring cells and induce the death of these neighboring cells.

The irradiated cells keep on secreting some signals, which are called bystander signals, and send them to the nearby nonirradiated ones. This may happen in two ways; the first one is gap junction, where the irradiated cell is connected with the nonirradiated cell by intercellular channels, these channels facilitate the mediating of intercellular communication between the cytoplasm of both cells, and these channels are called gap junction. The other way is a secreted soluble factor that sends signals to nearby cells (25).

These signals sent by the damaged cells can disrupt the neighboring bystander cells and causes cytogenetic damage, biochemical changes, and gene mutations which may persist in their progeny.

2.2 Tumors

Researchers develop treatments by understanding the difference between cancer and normal cells. Normal cells follow a particular cell cycle: They can grow, divide and die. In comparison to normal cells, cancer cells usually do not follow this typical cell cycle; instead of dying, they augment and produce more abnormal cells. There are many differences between normal and cancerous cells; next is about the key differences between the two cell types.

The first difference is mentioned in section (2.1.2.1) that some proteins, such as cyclins, control normal cell division. However, in the case of cancer cells, the control is lost by ignoring the body's signals to stop dividing, so these cells will divide abnormally. The second significant difference is that when normal cells die by the process of apoptosis, which is programmed cell death, then the dead cells are removed by this apoptosis process, for the cancer cells do not follow the programmed cell death; alternately, they follow necrosis with the uncontrolled release of the cell contents, and hence, they are going to cause inflammation in the surrounding tissue, this means they will affect the surrounding tissues negatively. Another major difference is that normal cells do not divide after a signal that triggers cell division is over. However, cancer cells keep on dividing even if this signal is over. The quick division of cancer cells prevents them from having the chance to differentiate, which is the opposite of normal cells, where these cells have distinct functions. An additional significant difference between the normal cells and the cancer cells is that the normal cells have contact inhibition. This regulatory mechanism keeps the cell growing into a single layer (a monolayer). So, if the cells have available space, they replicate rapidly and move freely until they occupy the entire space. At this point, the cells will stop replicating because they are coming in contact with each other, thereby the term contact inhibition. However, the cancer cells do not follow contact inhibition meaning that the cancer cells will not grow in a monolayer but in a multilayer. One more difference is that normal cells actually remain in place in the body; in other words, they will occupy a particular position in the body; on the other hand, cancer cells start spreading to other areas in the body, and these cancer cells are called metastatic

cancer cells. These are the main differences between cancer cells and normal cells. These variations create a microenvironment with characteristics that distinct from that in microenvironment in normal cells.

Several features of the tumor microenvironment, including acidosis, hypoxia, and aberrant vasculatures, have been identified (26, 27). This work will include a better understanding of how this microenvironment influences the behavior of cancer cells, cancer progression, and the regulation of cancer therapeutic responses; however, instead of studying all the hallmarks of the tumor microenvironment, this work will focus on the pH modifications since the acidity of the tumor microenvironment is a major characteristic of cancer cells that is generally related to the cell aggressiveness and invasiveness.

2.3 Acidic tumor microenvironment

An inclusive understanding of tumor microenvironment (TME), and its acidity will provide a conceptual chance to study the tumor survival, progression, and tumor response to treatment. The tumor microenvironment (TME) is a system that made up of the tumor itself as well as multiple normal, non-malignant cells around the tumor such as fibroblasts, blood cells, immune cells, and so on. In addition to the different cell components that is around the tumors also a non-cellular components such as extracellular matrix and exosomes (28).

Acidosis in the tumor microenvironment is a vital stress factor and selection force of cancer cell somatic evolution. Due to insufficient blood perfusion, hypoxia, inflammation, and glycolytic cell metabolism, the tumor microenvironment is acidic; the following paragraph describes where this acidity comes from.

In order to answer this question, the metabolic pathways that are altered between normal and cancer cells should be identified, starting by defining the metabolism. Term metabolism refers to a series of biochemical reactions that occurs within the living organism to maintain the living condition of the cells inside it. Metabolic pathways can be of two varieties: catabolism or anabolism. Catabolism mostly breaks down larger molecules into smaller pieces, releasing energy in this metabolic process. Anabolic process, small organic molecules are assembled into a larger ones, metabolic process requires energy to occur; this metabolic pathway can be called a biosynthetic pathway

because this way synthesizes the ingredient necessary for the structure and proper functioning of the cell. The catabolic reactions provide the energy for anabolic reactions. This energy can be stored in cells as ATP (adenosine triphosphate). Nearly all organisms depend on the breaking down of glucose to provide energy to their cells, and this process is called glycolysis. Glycolysis reaction takes place in the cytoplasm of the cell. This is the process by which glucose molecule is split into two pieces called pyruvate. Glycolysis is the starting point for two main processes to produce ATP: aerobic respiration (mitochondrial respiration) and fermentation (anaerobic glycolysis). The use of one of the processes to create ATP depends on the presence or absence of oxygen and the cell's proliferation level.

Aerobic respiration in cells takes place when oxygen is present, where cells break down glucose to produce pyruvate in the cytoplasm as mentioned above in the glycolysis reaction; after entering the produced pyruvate into the mitochondrial matrix, it is completely oxidized during the Krebs cycle (or citric acid cycle) giving ATP, NADH (Nicotinamide adenine dinucleotide), and FADH2 (Flavin adenine dinucleotide) molecules, NADH and FADH2 are then utilized during electron transport chain that is the last step of aerobic respiration, this known as oxidative phosphorylation (OXPHOS). Aerobic respiration produces carbon dioxide (CO_2), water (H_2O), and energy stored as ATP molecules. This reaction allows maximum ATP production and limited lactate production (an ionized form of lactic acid). The following is a summary of the interactions that happen during aerobic respiration and the total value of ATP molecules for each glucose molecule:

1- 1 glucose ——— 2 pyruvate + 2 ATP (Glycosis)

2- 2 pyruvate ——— 2 ATP + 6 NADH + 2 $FADH_2$ (Krebs cycle)

3- 6 NADH and 2 $FADH_2$ molecules that can go on to the electron transport chain, which gives 26-28 ATP

So, this results in an energy gain of about 36 ATP per glucose.

Contrarily, if the cells do not have enough oxygen present, they go through anaerobic glycolysis; in this reaction, the pyruvate produced from glycolysis is transformed into lactate acid; this happens because the produced pyruvate will not feed into the Krebs cycle

instead it will be directly reduced by NADH to produce lactate. This reaction produces little amount of ATP and a large amount of lactate.

1- 1 glucose ——— 2 pyruvate + 2 ATP (Glycolysis)

2- 2 pyruvate ——— 2 lactate acid (Lactate fermentation)

Note that ATP per mole of glucose produced by anaerobic glycolysis is less than that produced by OXPHOS. However, it permits a more rapid generation of ATP than OXPHOS (29).Fig. (A.6) summarize the two metabolic pathways with their branches.

In the case of tumor cells, as known, cancer cells are highly proliferative, so they need energy, and this energy is produced by breaking down glucose, so cancer cells are famous for their high glucose consumption. A metabolic phenomenon was discovered by a physiologist Otto Warburg, and this effect was observed in cancer cells; Warburg noted that cancer cells switch their metabolism from aerobic respiration to anaerobic glycolysis. In other words, they convert glucose to lactate even when there is enough oxygen to support oxidative phosphorylation (30, 31).

Already been stated that oxygen levels play an essential role in ATP production since it is used in the final step in mitochondrial respiration. In order to supply the cells with the optimal amount of oxygen, the presence of vessels is necessary. Oxygen can diffuse from the blood vessel up to a distance of approximately 75 μm (32). In rapidly growing tumors, the consumption of oxygen is very high; if the tumor expands further, this leads the cell to run out of oxygen resources and become hypoxic; in order to avoid hypoxia, tumors may induce the growth of new blood vessels, which deliver oxygen and other nutrients then the tumor is vascularized, the creation of new blood vessels from the existing ones and this process called angiogenesis.

In general, hypoxia has a negative impact on the cancer cells because of the absence of oxygen. However, cancer cells have the ability to accommodate this condition by activating an oxygen-responsive signaling pathway known as the Hypoxia-Inducible Factor (HIF). HIF can shift the ATP production process from OXPHOS to anaerobic glycolysis due to low O_2 levels.

Now, because of the unique glycolytic activity in the hypoxic cancer cells, they excrete large quantities of lactate and H+ ions (protons) due to Lactate Dehydrogenase (LDH) because in an aqueous environment, as in cytosol, H+ easily dissociate from lactic acid and this results in the formation of lactate. So, with anaerobic glycolysis, the amount of lactate and the amount of H+ in the cytosol increase, and this increasing of H+ will make intracellular pH more acidic, and the acidity of the intracellular environment is cytotoxic through the apoptosis induction (33). In order to maintain the pHi value within the physiological level (7.0–7.2), cancer cells export lactate and H+ ions into extracellular space. This implies a decrease in extracellular pH (pHe) value leading to acidification of the tumor microenvironment. So, in cancer cells, a reversed pH gradient (pHi > pHe) is formed in contrast with normal physiological conditions (pHi < pHe). The export of protons and lactic acid from tumor cells into extracellular space is done via acid-base regulators such as Na+/H+ exchangers (NHEs), which permit the entry of Na+ ions in exchange for the release of an H+ ion. In addition to this, monocarboxylate transporters or Proton-lactate transporters (MCTs) have been proposed to be suitable transporters to maintain regular pHi, where these transporters are electroneutral allow the transmission of monocarboxylic acids such as lactate or pyruvate through cellular membrane, the Proton-lactate transporters move a monocarboxylic acid together with the transport of a proton with the same quantities (34).

The reversed pH gradient encourage cancer progression, via the fairly acidic pHe can facilitate degradation of the extracellular matrix (ECM) and that occur when the cancer cell secreted some enzymes such as matrix metalloproteases (MMPs) and cathepsins in which these enzymes are activated in acidic environment, and the activation of these enzymes allows the degradation of ECM, and hence, it helps the cancer cells to spread and infiltrate the surrounding tissues. Accordingly, extracellular acidity induces invasion and migration (35, 36). Alkaline pHi also has effects on cancer cell function such as limiting apoptosis, and hence, promoting cell survival, increasing proliferation (37).

2.4 Glioma

Gliomas are the most common malignant (cancerous) in the brain and spinal cord, in particular in the gluey supportive cells (glial cells) that surround nerve cells and help them function. The brain has stem cells, these stem cells can give off daughter cells, and these cells can become essentially one of four types of cells: neurons, which are the basic

building blocks of the nervous system, astrocyte is the star-shaped glial cells that inhabit in the brain and spinal cord. They are the most numerous cells in the human brain; oligodendrocyte glial cells that are responsible for producing a fatty protein called myelin, which insulates axons; the long extensions of nerve cells (neurons), and ependymal cells are specific glial cells that line the Cerebrospinal Fluid (CSF)-filled ventricles (an area where fluid is contained in the brain) in the brain, and the central canal of the spinal cord. Glioma brain tumors can arise from astrocytes, oligodendrocytes, or ependymal cells when these cells grow out of control. Glioma comprises about 30% of all brain tumors, and central nervous system tumors also account for almost 80% of primary malignant brain tumors (38).

2.4.1 Classification of glioma

Gliomas are malignant (cancerous) and can proliferate and diffuse but don't usually spread beyond the central nervous system. However, they are life-threatening because they can be hard to reach and treat with surgery or grow into other brain areas, Fig.(A.7). Unlike other cancers characterized by the stage, gliomas have a different classification system based on grade, which measures how aggressive the tumor is. On the bases of their histological characteristics, aggressiveness, and proliferation rate, they have been assigned by World Health Organization (WHO) grades I to IV, which are categorized as low-grade or high-grade, and these grades show malignant degrees:

1. Low-Grade Glioma

- Grade I. These tumors are rare tumors found most frequently in children. Moreover, have lower proliferation rates, and they are most likely to be benign. They can often be cured with surgery. A juvenile pilocytic astrocytoma is an example of a Grade I glioma.
- Grade II. These types of tumors are less likely to grow and have a low level of proliferative activity but are more likely to recur after treatment. Astrocytomas and oligodendrogliomas are the familiar grade II gliomas.

2. High-Grade Glioma

- Grade III. These tumors are more likely to have speedily dividing cells. They can proliferate. Grade III gliomas include anaplastic astrocytomas and anaplastic oligodendrogliomas.

- Grade IV. Cells are actively dividing in a grade IV tumor, and the proliferation rate is very high. In addition, the tumor has to be more aggressive. Grade IV gliomas are called glioblastomas.

Recently, World Health Organization (WHO) classified glioma due to its DNA mutation (39). The classification of glioma types is a key diagnostic process because it helps the therapies guide the treatment journey.

Table 2.1

Summary of (WHO) classification of glioma

The classification of glioma	Low grade glioma	Grade I	Pilocytic astrocytoma
		Grade II	Astrocytomas and oligodendrogliomas
	High grade glioma	Grade III	Anaplastic astrocytomas and anaplastic oligodendrogliomas.
		Grade IV	Glioblastomas.

2.4.2 Glioma treatments

Treatment options include surgery, radiation therapy, chemotherapy, and targeted therapy will be chosen according to the type of glioma. For a low-grade brain tumor, surgery may be the only treatment needed, especially if all of the tumors can be removed, but if there are visible parts of the tumor that may remain after the surgery, then radiotherapy or chemotherapy are proposed. Treatment for higher-grade tumors usually begins with surgery, radiation therapy, and chemotherapy (40).

Table 2.2

Treatment techniques for different types of gliomas

Type of glioma	Treatment
Pilocytic astrocytoma (WHO Grade I)	Surgical resection
Astrocytoma (WHO Grade II)	Surgical resection (or biopsy) or Radiotherapy
Anaplastic astrocytoma, Oligodendroglioma/Oligoastrocytoma (WHO Grade III)	Surgical resection (or biopsy) and Chemotherapy (or Radiotherapy)
Glioblastoma (WHO Grade IV)	Surgical resection (or biopsy), and Radiotherapy and Chemotherapy (Temozolomide)

Radiotherapy is the dominant form of therapy because it controls tumor growth, improves progression-free survival, and maintains patient quality of life by reducing the risk of seizures and delaying anaplastic transformation.

Chapter Three
Materials and Methodology

3.1 Materials

3.1.1 The F98 cell line

The in-vitro experiments are essential to study the efficacy of novel therapeutic techniques for tumors. They are often the first stage in testing for new treatment protocols before they are given to humans. For instance, implantation of a micro-tumor created in vitro in a small animal allows for more reproducible assessment of therapy impact and tumor progression. So, cell cultures (primary cells and cell lines), organs, tissues, or animals are inserted in particular environmental conditions close to those in vivo to use them to study the progression of cancer. For glioma, different Rat models such as the 9L,C6 T9, RG2, F98, BT4C, RT-2, and CNS-1 gliomas have been commonly used in neuro-oncology research for over 30 years because they are applied to develop inventive therapeutic agents and test the effectiveness of diagnostic modalities. So, in our study, we used one of these models called the F98 glioma rat cell line (rat, ATCC® CRL-2397). This rat F98 glioma cell line is deposited in a monolayer in two dimensions (41).

In 1971 this cell line was established by W. Wechsler (in Dr. A. Koestner's laboratory, Ohio State University). Initially, the F98 glioma was induced by injecting a small dose of N-ethyl-N-nitrosourea or ethylnitrosourea (ENU) into pregnant rats, which developed spontaneous tumors in the progeny of which were isolated and subsequently were propagated in vitro and cloned. The F98 cell line was an excellent choice due to its invasive growth pattern within the tissues, and they are poorly immunogenic, making it closer to human gliomas (42). This cell line is kept in a Dewar of liquid Nitrogen (–196 °C) to allow long-term storage of the cells. This cell line is deposited as a monolayer in two dimensions in our experiments.

3.2 Cell culture conditions

First, the cell cultures are carried out in a dedicated clean room. The cell line was maintained and passaged in a medium composed of Gibco™ DMEM medium (Life Technologies SAS, Courtaboeuf, France) with 4.5% glucose supplemented with other

This section is considered as a useful procedure for physics students.

components such as:

1. 10% fetal bovine serum: It contains growth factors.
2. 1% sodium pyruvate: used as an additional energy source.
3. 1% HEPES buffer solution (Optional): It maintains a balanced pH value in the media.
4. 1% GlutaMAX™.
5. 1% penicillin-streptomycin: It is an antibiotic to prevent bacterial contamination.

DMEM contains phenol red as a pH indicator. The color of phenol red turns to yellow for low pH values and turns to bright pink when the pH is high.

This nutrient medium provides a healthy environment, maintains optimal cell performance, and reduces the possibility of microbial contamination. The cells are set inside flasks and placed in a carefully controlled atmosphere incubator that provides the right growth conditions, such as temperature, CO_2, and degree of humidity. Generally, the incubator is set at a temperature of 37°C, 95% air, and 5% carbon dioxide CO_2, see Fig. (B.1)

3.3 Cell Handling

3.3.1 Cell trypsinization and passaging

The F98 cells are seeded in a 75 cm^2 culture flask containing 10 mL of the nutrient medium and continuously incubated at 37 °C and 5% CO_2 so they can attach to the bottom surface of the culture flask and start dividing and growing to cover the entire surface. Once the flask becomes crowded, the cells need to be split to two flasks, so the cells will have enough space to keep dividing. This operation is called cell subculture or cell passaging. These cells are subcultured about twice a week: Following their incubation, the cells are detached with 1 mL of 0.05% trypsin-EDTA solution and incubated for 5 min. Then we stopped the action of trypsin by applying the medium with the same volume as trypsin, and then we reseeded the cells with a lower concentration in new flasks to use them in our experiments.

3.3.2 Cell counting*

The different cell culture experiments usually require knowing the number of cells that will be used. There is a different way to perform cell counting. The automated cell counter

(Countess II FL) was used in our project. This counter is supplied with slides that contain two enclosed chambers to measure two different samples or perform replicates of the same

*This section is considered as a useful procedure for physics students.

sample. The cells to be counted are loaded into the instrument by inserting the slide into the slide carrier inserted in the slide port until it is completely inserted. Then we press (capture), which appears on the screen. Within 10 seconds, it gives the cell count addition to this, it provides other information such as live and dead cell concentration/mL, cell viability, cell images, and cell size (43).

3.4 Fluorescence Microscopy

Despite the techniques that appeared in the last fifty years to view the surface of objects down to the atomic level, such as scanning tunneling microscopy and atomic force microscopy, fluorescence microscopy established itself to detect particular elements of complex biomolecular assemblies. Fluorescence microscopy is an imaging method that visualizes possible fluorescence of materials and molecules. This technique has become an essential tool in biology and biomedical research.

Most cellular components are colorless and hard to distinguish, so fluorescent dyes known as fluorophores are used to label and stain these components. We obtain images with good contrast by exciting these fluorophores at the proper wavelength.

3.4.1 Principle of fluorescence

In 1852 a British scientist Sir George G. Stokes, first introduced the phenomenon of fluorescence when he observed that the mineral fluorite (CaF_2) was illuminated by ultraviolet light. It emitted a red light. From his experiments with a wide range of materials, Stokes concluded that some substances could convert ultraviolet light, which is invisible, to visible light with a longer wavelength (later known as Stokes low) (44).

Nowadays, fluorescence can be defined as the immediate emission of light by fluorescent molecules (a fluorophore) after they absorb electromagnetic radiation.

The fluorescence process is illustrated by an electronic transitions diagram called Jablonski diagram, as in Fig. (A.8)(45). As we see, the fluorescence goes under three stages; the first one starts when the fluorophore absorbs an excitation radiation from an external source such as a laser or an incandescent lamp and the amount of this excitation energy is equal to $E_{EX} = h\,\nu_{EX}$ where h is planck constant = 6.626070×10^{-34} J.s and ν_{EX} is the frequency of the excited radiation. This energy induces electrons passage quickly

from the ground electronic level S_0 to the excited level S_2. We should know that the excited energy is at least equal to the energy difference between S_0 and S_2. This explains that there is energy below which it cannot excite the fluorophore. In the second stage,

*This section is considered as a useful procedure for physics students.

the excited electrons in the state S_2 go to the more stable excited level S_1 by dissipating some of their energy due to the interactions within the surrounding environment. This phenomenon is usually called internal conversion, lasting about 10^{-12} seconds. The electron will return to the ground level via a competitive process. Either the electron relaxed directly to S_0, yielding the emission of a photon with energy $E_{EM} = h\,\nu_{EM}$ which is the case for fluorescence as the last step in Fig. (A.8) and lasts from 10^{-12} sec to 10^{-8} sec and the energy of the emitted photon is smaller than the energy of the absorbed photon because of the internal conversion. Or it will pass to S_0 because of the loss of the energy as nonradiative energy such as heat in the medium. The final probability for the electron is to pass from S_1 to T_1 due to the intersystem conversion and then from T_1 to S_0, and this phenomenon is called phosphorescence (46). Our research will only focus on fluorescence since it is a rapid (occurs within nanoseconds) conversion of absorbed radiation into re-emitted energy.

3.4.2 Fluorescence Microscope

In the early twentieth century, Oskar Heimstaedt, Heinrich Lehmann, August Köhler, Carl Reichert, and others developed the fluorescence microscope that uses fluorescence properties to study the characteristics of organic or inorganic substances. At first, a problem appeared that the produced images looked blurry, with low resolution, since the fluorescence observed comes from the plane of focus and all parts of the specimen when irradiated with the exciting light. In 1957, Marvin Minsky presented a simple solution to overcome these parasitic fluorescences by placing an element called a pinhole between the path of the excitation and emission light beams, and this will eliminate the fluorescence signals that have not been emitted from the plane of focus, this technology is now known as confocal microscopy (47, 48).

If we follow the light path in Fig.(A.9)(49), the excitation light (green line)produced from a light source such as a laser, LED then this light will be reflected by a dichroic mirror (Beam splitter); this type of mirror reflects the light shorter than a given wavelength and

passes the light longer than that wavelength. After the dichroic mirror reflects the light, the beam will pass the objective lens and hit the specimen to excite the fluorophores. The objective will collect the fluorescence emitted (red line) by fluorophores. It will cross the dichroic mirror, and the pinhole will eliminate part of the light before arriving on the detector.

3.4.3 Fluorophores

A fluorophore is a chemical compound with fluorescence properties that can re-emit light upon light absorption (excitation). Due to its shift in wavelength between excitation and emission (Stokes shift), the fluorophore has asserted itself as a main tool used to increase the technical improvement in fluorescence microscopy, particularly in observing living organisms.

The main characteristic we considered to study the fluorophore is to realize the excitation and emission spectra. Fluorophores can absorb light with a fixed wavelength and give light within a range of wavelengths, and this happens when the excited fluorophore releases the photons during the transition towards the different resonance levels of the ground state. This is how we obtain the emission spectra. The excitation spectra are acquired by observing at one wavelength the fluorescence intensity as a function of the excitation wavelength. In addition to this characteristic, we must consider the imaging instrument capabilities (such as filters and excitation lasers) and the phenomena that will be studied in order to choose which fluorophore will be used. Different types of fluorophores can be classified into categories such as organic fluorophores, fluorescent proteins, and quantum dots.

The different fluorophores used in our project are:

1- Resazurin (7-Hydroxy-3H-phenoxazin-3-one 10-oxide)

It is a reagent used to determine cell viability and study cell metabolism, also known as Alamar Blue. Resazurin is not fluorescent, but in metabolically active cells undergoing aerobic respiration, resazurin is converted to resorufin, which is highly fluorescent. When we add the resazurin to the medium with cells, live cells continuously reduce resazurin to resorufin, which turns the media from blue to pink and emits red fluorescence. Therefore, the cell viability could be detected using a microplate reader. In our experiment, to determine the cell viability, a 1/20th volume of resazurin was added directly to the cells

in the culture medium, then we incubated them for 2-3 hours at 37ºC, 5% CO_2 in the incubator. After that, the microplate reader is used to measure how fluorescent the medium is, which is the indicator of how much we have active cells in this medium (more fluorescence, more active cells)

2- Carboxy SNARF-1-AM (seminaphtorhodafluor-1-acetoxymethylester):
It is a cell-permeant stain that can be used to determine the intracellular pH in our glioma cell. This version of Carboxy SNARF-1 is not fluorescent and has an acetoxymethyl ester (AM) group making the compound neutral and allowing it to cross the cell membrane. Once it enters the cell, intracellular esterases will cleave the ester group of the molecule, releasing the negatively charged probe and trapping the probe in the cytoplasm, making it potentially fluorescent.

Carboxy SNARF-1 was widely used to evaluate internal pH (50). It has a pKa of ~7.5, so it exhibits a notable pH-dependent emission shift from yellow-orange to deep red fluorescence under acidic and basic conditions. Thus, at pH values below its pKa, the probe predominates in a protonated state and exhibits maximum fluorescence emission at ~ 580 nm when excited at 488 nm. Whereas, at pH values above the pKa, it exhibits maximum fluorescence emission at ~ 640 nm when excited at 488 nm as showed in Figure. (A.10). Shift obtained between the spectra can be used to perform a ratiometric measurement for more accurate pH determinations.

The probe is supplied as a lyophilized solid containing 50 µg and is provided in sets of 10 × 50 µg vials of lyophilized solid. Then the stock solution of SNARF-1-AM is prepared at 1 mM of high-quality anhydrous dimethylsulfoxide (DMSO). After adding the probe to the cells in a culture medium, they were placed into the incubator at 37ºC, 5% CO_2, for 30 min. Once loaded with the probe, cells were washed to remove the probe not taken up by the cells, and a new fresh medium was added (51).

3.4.3 Image processing

In this project, we used the confocal Eclipse Ts2R-FL Nikon microscope (Scop Pro, Marolles-en-Hurepoix, France). It is an inverted microscope with the objective lens facing upward to view the sample from below. Also, this microscope uses high intensity LED light source illuminator. This microscope has a cage incubator for finely controlling temperature (37º C), humidity, and CO_2 supply. Also, it is equipped with an ORCA-

Flash4.0 LT Digital CMOS camera (Hamamatsu city, Japan) and CellSens acquisition software, see Fig. (B.2).

The images produced from experiments were performed with the Fiji software. Fiji is an open-source image processing package based on ImageJ. Fiji macros were developed to detect cells in experiments. Also, Python was used for further analysis of the data.

3.4.4 Fluorescence microplate reader (microplate fluorometer)

It is an instrument capable of measuring the fluorescence emitted by analytes in a well of a microplate and detecting absorbance and luminescence. Fluorescence plate readers are helpful due to their ability to measure multiple wells in a single run, so it saves time and offers accurate measurement of any fluorescence intensity assay. A Fluorescence microplate reader usually contains a light source for selecting excitation light (i.e., monochromators and/or filters) and also includes a second optical system for selecting emission light and a detector.

The microplate reader used in the laboratory is the Fluoroskan Ascent FL microplate reader equipped with Fluoroskan software, see Figure. (B.3).

3.5 The GSR D1 Gamma Irradiator

All the experiments done in the project use the primary source of radiation: The GSR D1 Gamma Irradiator (GSR D1, Gamma-Service Medical GmbH, Leipzig, Germany), see Figure. (B.4). It is a self-shielded irradiator that uses gamma radiation in radiobiological research, i.e., it is used to irradiate organic and non-organic materials. It has four sources of Caesium-137 (Cs^{137}) as a gamma source, a radioactive isotope formed as a joint product of the nuclear fission of radioactive materials, such as uranium and plutonium. This radionuclide has a comparatively long half-life time of about 30 years. This isotope is formed artificially in nuclear weapon tests, nuclear reactors, and nuclear accidents.

Figure. (A.11) shows how Cs-137 produces gamma radiation, the radioactive decay of Cs-137 has two probabilities. First, with a high probability, the Cs-137 goes through a two-stage process. Initially, it goes through beta decay to produce short-lived Barium (Ba-137). Ba-137 emits gamma radiation within seconds with an energy of 661.66 KeV due to the transition to stable Ba-137. The second probability is that it undergoes beat decay directly when it transmits to stable Ba-137 (52).

The one with large probability

$$_{55}Cs^{137} \longrightarrow {}_{56}Ba^{*137} \quad (3.1)$$

Then

$$_{56}Ba^{*137} \longrightarrow {}_{56}Ba^{137} + \gamma\ (661.66\ KeV) \quad (3.2)$$

The second with low probability

$$_{55}Cs^{137} \longrightarrow {}_{56}Ba^{137} + \beta^{-}\ (1174\ KeV) + \bar{\nu}_{e} \quad (3.3)$$

3.6 Preparing the pH solutions

At the beginning of our project, DPES solutions were used to prepare different solutions with different pH values. However, we faced a problem when we needed to prepare solutions with a wide range of pH values by adding drops of HCl and NaOH. The pH values fluctuated very quickly, so we could not handle them, so we chose to prepare our own buffer solution and then obtained a wide range of pH solutions by adding HCl and NaOH.

Two buffer solutions were prepared. Solution (1) contains 10 mM Hepes, 145 mM NaCl, 5 mM KCL, 5 mM dextrose (Glucose), 1 mM $CaCl_2$, 1 mM $NaH_2PO_4.H_2O$, and 0.5 mM $MgSO_4$ below a schematic shows how we prepared this solution. First, this solution was adjusted to pH= 7.4 as a regular solution. Then we prepared solutions with various pH values from 5- 8.5 by step equal to 0.5 by adding 1.5 M of HCl and 0.5 M of NaOH, and the pH changes followed with a Thermo Scientific Orion 3-Star Benchtop pH meter. The second buffer solution, Solution (2) contains 10 mM Hepes, 20 mM NaCl, 130 mM KCl, 5 mM dextrose (Glucose), 1 mM $CaCl_2$, 1mM $NaH_2PO_4.H_2O$, and 0.5 mM $MgSO_4$ then this solution adjusted to prepare the same pH values from 5- 8.5 by step equal to 0.5, same as mentioned before (54).

Preparation: we will start adjusting the pH values for the two solutions using the Thermo Scientific Orion 3-Star Benchtop pH meter, but first, we needed to calibrate it. Two buffer solutions with known pH values (pH=4.01 and pH=7.01) were used for pH calibration. The electrode is rinsed with distilled water to start the calibration and placed into the first buffer. We waited till the pH meter stopped flashing and gave a relative value to the value of the buffer. Then, the electrode is put in the second buffer solution to proceed to the next

calibration point after rinsing it with water and waiting till we get the second value. The slope was saved, and ended the calibration.

Initially, the regular solution was adjusted by adding a few drops of HCl and NaOH (1). With a magnetic stirrer's assistance, MR Hei-Standard's solution was perfectly mixed after adding the HCl and NaOH. Once the first value was obtained, we put a small amount of the solution with pH=7.4 in a small bottle, and then the electrode was rinsed and placed in the solution to get the other pH values. The pH values were adjusted in the same way as before. It ended up preparing 9 different values of solution (1), the regular one equal 7.4 and the other values (5, 5.5, 6, 6.5, 7, 7.5, 8, and 8.5) and 8 different values of solution (2). Dissolve all materials in one liter of water.

Scheme 3.1

Preparing the pH solutions

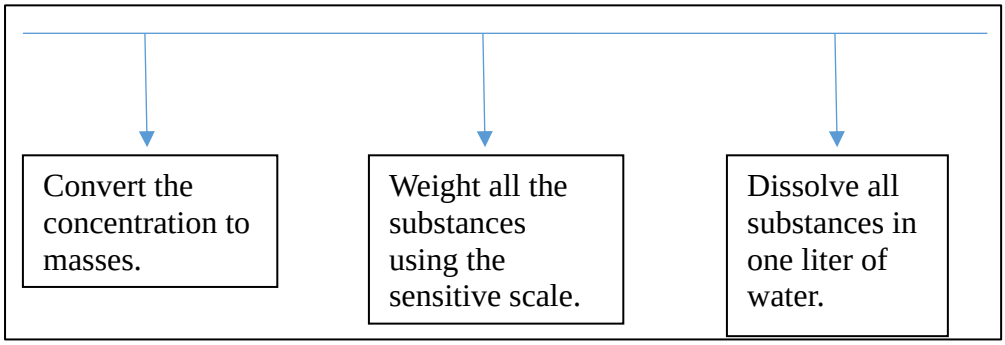

Figure 3.1

The setup of pH solution preparation

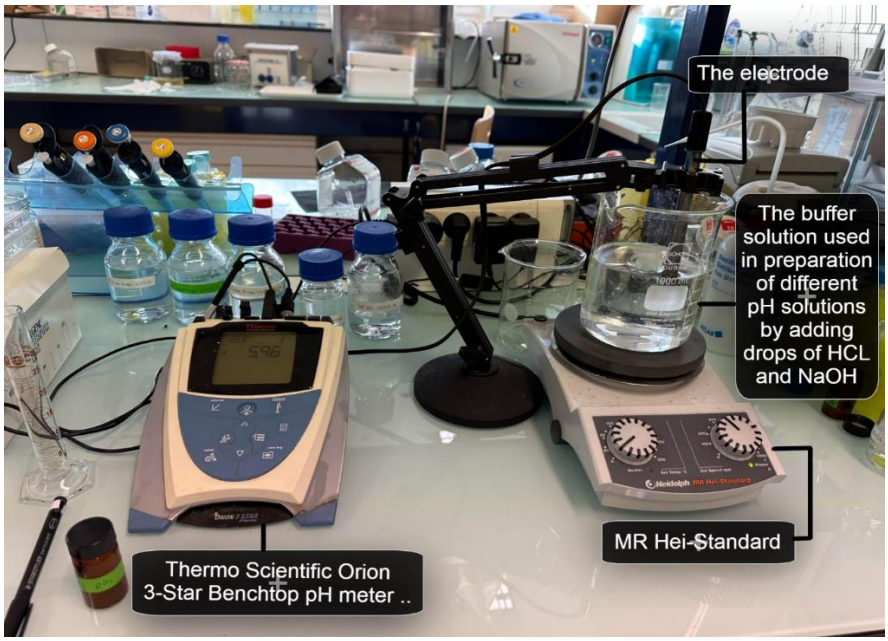

3.7 Time lapse microscopy to study the cell proliferation

5×10^{4} cells/mL of Red-F98 cells were seeded on day0 (D0) onto 6-well plate in 3mL of standard cell culture medium 24 h before the experiment. On day 1 (D1), we replaced the medium with DPES solution with different pH values, i.e., pHe 6.2, 7.1, 8.2, 2 h before radiation. For radiation, Dose=15 Gy was used to irradiate the cells. After radiation, the irradiated cells were kept in the same pH solutions for 2 hours before these solutions were replaced with 3mL of fresh culture medium. The fluorescence microscope and the CellSens acquisition software were used to collect the data by taking images of each well every 30 min for 7 day, and hence, these images are fluorescence because the cell contains a specific type of fluorophore that already loaded inside the cells, so the fluorophore absorbs the electromagnetic radiation produced by the microscope and then it emits radiation which will be detected by the microscope, and then produces fluorescence images which saved as a short video.

Scheme 3.2

The time line of the time-lapse experiment

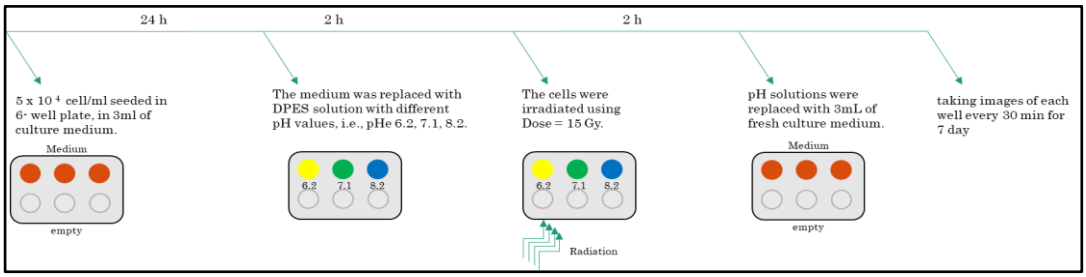

Fluorescence images of irradiated Red- F98 glioma cells were analyzed with ImageJ/Fiji software using (Find Maxima) function, which is used to select local maxima in each fluorescent image, in other words, to find prominent points within the images, and this done via setting the function's parameters such as the (prominence) here the value of prominence chosen in order to select the point with intensity's values equal and larger than the prominence value. The prominence should be suitable for all the images and make sure the all the cells are counted during this process. Then with Python, we can plot the number of cells with time.

Figure 3.2

Analysing the images using ImageJ/Fiji

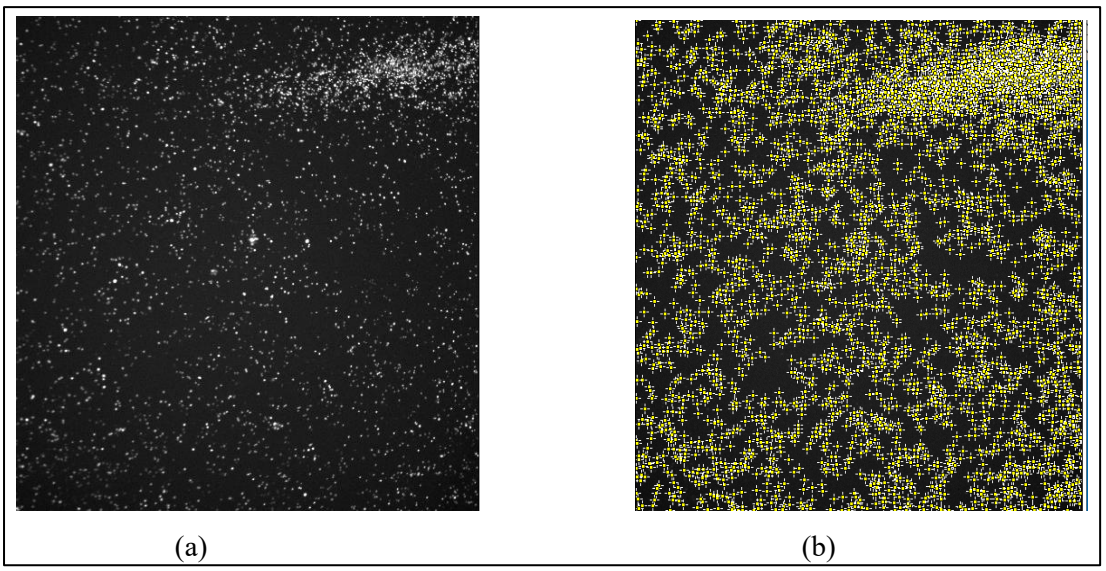

A real image of the cells that has been taken by the microscope. (b)The same image but after applying the function (Find Maxima) to count the cells.

3.8 The methodology of the cell viability experiment

$5x10^4$ cells/ml of F98 cells were seeded on day0 (D0) onto 48-well plates in 500µL of standard cell culture medium 24 h before experiment. 4 plates were prepared each for different radiation doses (0 Gy (As a control cell culture), 10 Gy, 20 Gy, and 30 Gy). On day 1 (D1), the medium was replaced with different pH values solutions prepared from solution (1). After 2 h, the cells were irradiated, then the pH solutions were replaced with a fresh culture medium. After 48 h of incubating the cells in 5% CO2 and 37º C and waiting for the effect of radiation to appear, a 1/20th volume of resazurin was added to the cells and waited for 2-3 h. During this time, live cells will reduce resazurin (not fluorescent) to resorufin (fluorescent), making the medium fluorescent. A Fluoroskan Ascent FL microplate reader was equipped with Fluoroskan Ascent software (version 2.4) to collect the data. The software provides complete data handling and controls the reader functions. First, a new session was opened for a 48-well microplate, and then the occupied wells were selected. Then the instructions were applied for the reader to measure the fluorescence intensity for the selected wells. Resorufin was excited using wavelength at 575 nm, and the fluorescence emission was recorded at 590 nm. Then the fluorescence intensity of the medium in each well was recorded, and this data was saved on excel sheets. The data analysis was performed using Python.

Scheme 3.3

The time line of cell viability experiment

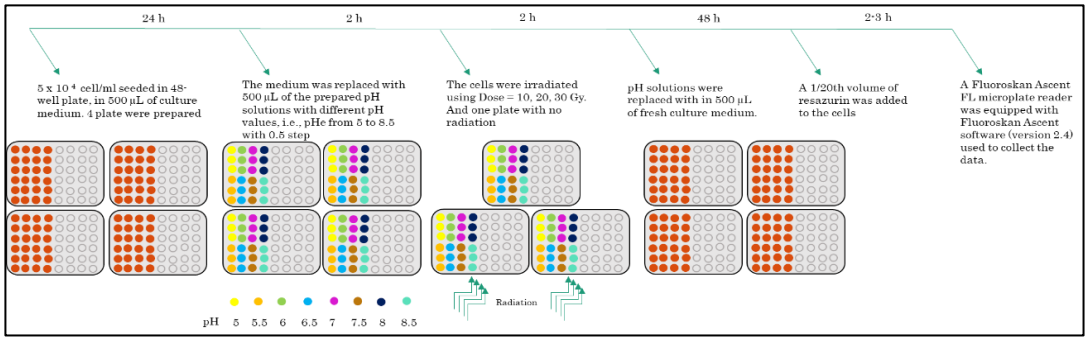

3.9 The methodology of the intracellular pH measurements

$5x10^4$ cells/ml of F98 cells were seeded on day0 (D0) onto 48-well plates in 500µL of standard cell culture medium 24 h before the experiment, 4 plates were prepared for the experiment:

1. One plate will not be irradiated dose= 0Gy
2. Three plates will be irradiated for different doses 10 Gy, 20 Gy, and 30 Gy.

Two rows of the plate of dose = 0 Gy will be used to get the calibration curve, and the other two rows to measure pHi for the non-irradiated cells. The other plates, two rows each, were used for the rest of the experiment. On the following day (D1), 2 h before the radiation, the culture medium was replaced with 500µL of the prepared pH solutions in section() (Solution (1) and solution (2)). These solutions were arranged in the wells as follows: For the 0 Gy plate, the pH solutions from solution (2) were used for the calibration curve experiment, for the other 2 rows in this plate in addition to the other three plates, the pH solutions from solution (1) were used.

After radiation, the irradiated cells were kept in the pH solutions for 2 h. Next, 2 µM SNARF-1-AM from a 1 mM stock-solution in DMSO was loaded into cells. As a reminder, once inside the cell, the ester is supposed to be hydrolyzed by intracellular esterases, releasing the charged probe, which is fluorescent and unable to permeate the membrane. In that way, it is trapped inside the cell. After 40 min incubation with SNARF-1, cells were washed with fresh pH solutions arranged as before to remove the probes not taken by the cells and avoid the background noise in the images. However, only for the calibration curve experiment two other substances were added after washing the cells with fresh pH solutions from solution (2) to the wells, which are (0.3 µl) nigericin and (0.5 µl)

valinomycin (more details will be described in the coming sections). Finally, the images have been taking using the fluorescence microscope.

Scheme 3.4

The time line of cell viability experiment

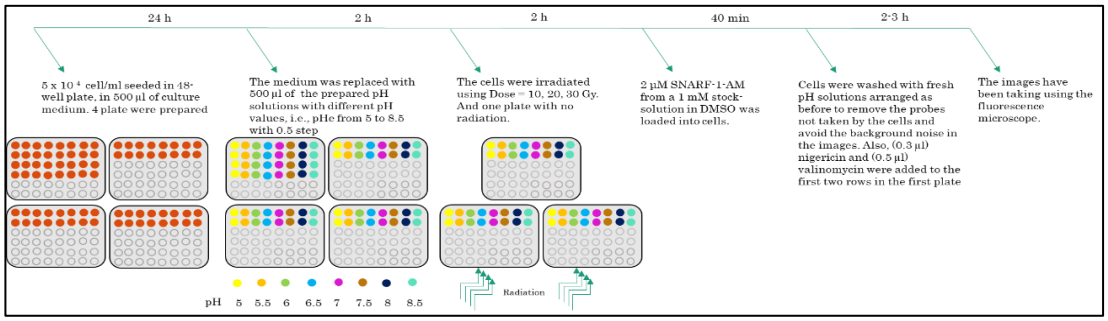

Chapter Four
Results and Discussion

4.1 Extracellular pH as a therapeutic target to optimize the efficacy of radiotherapy

4.1.1 Cell Proliferation

A detailed understanding of the effect of the radiation on a cell population placed in different pH solutions will be presented in this section. As reported in previous sections, radiation can inhibit mitosis by causing damage to the DNA of the cells, meaning it will indefinitely inhibit the cell's ability to divide and proliferate. In contrast, some of the injured cells might have the ability to recover from DNA damage. In short, when a cell is irradiated, it can either repair and continue to function or cause small changes leading to mutation or death.

Beside the effect of radiation on the DNA of cells, this effect may be affected by changing the acidity of the cell's medium since the change in microenvironmental pH is one of the remarkable stress-inducing events in cancer (55).

In order to test the effect of radiotherapy combined with cell culture medium pH modifications, the proliferation of the irradiated F98 cell culture placed in different pH was followed using the microscope in time-lapse mode and taking pictures every day to see if adding the pH parameter will affect the efficiency of radiation therapy.

After following the methodology of the experiment in section (3.7) we obtained the results appears in fig. (4.1)

Fig.(4.1) shows the dependence of radiation on the pH_e of the medium itself. The two plots are for the same experiment. The first is the number of cells obtained using the Fiji software with time in hours, and the second is the normalized number of cells) with time in hours to understand the results better. Normalization done by dividing all the values of counts at any time (t) by the value of the count at (t_0). If we generally look at the two plots, the curves showed the same behavior when the cells in different pH solutions were exposed to the same radiation dose.

Figure 4.1

Cell proliferation results

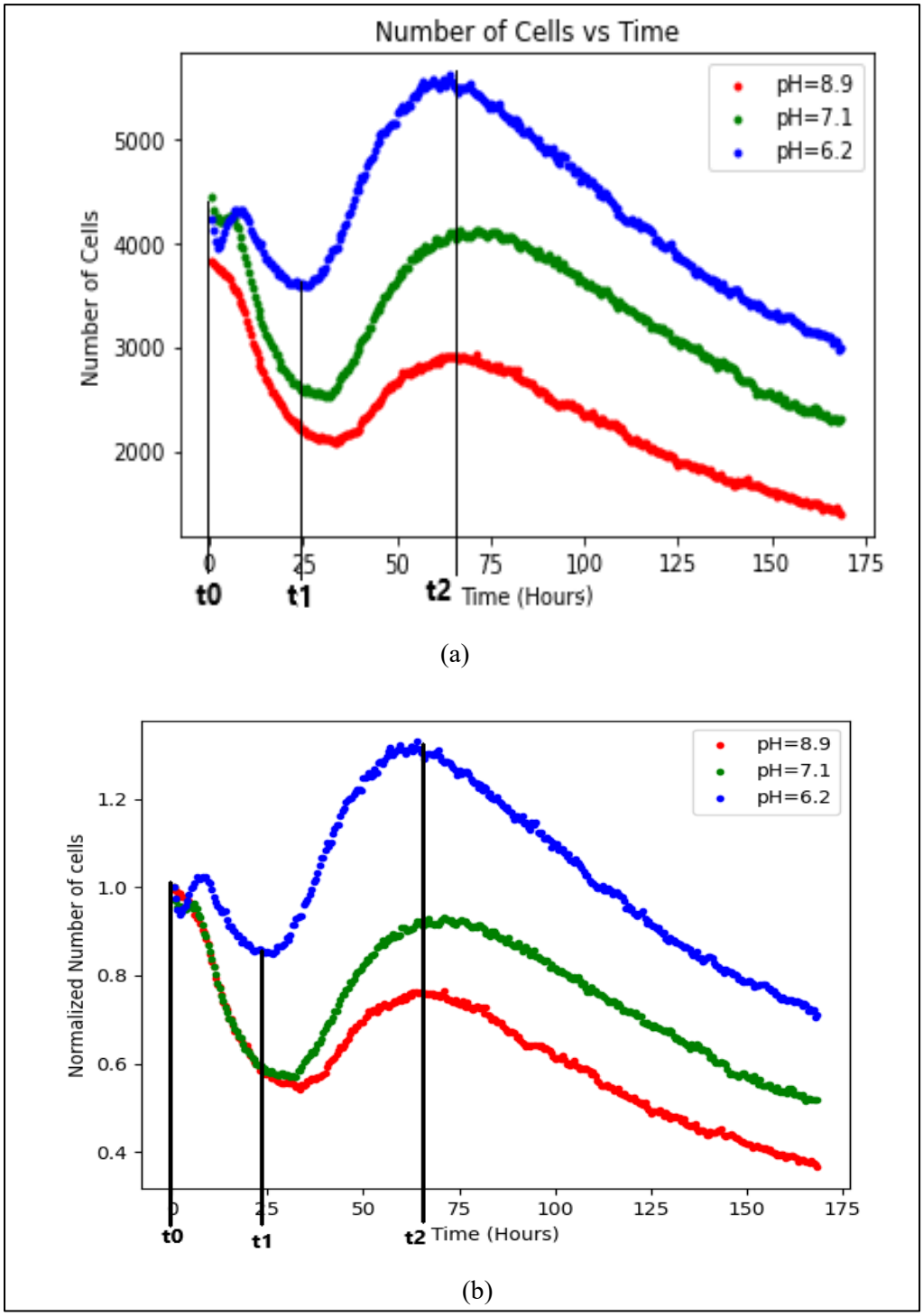

(a) represent the number of cells vs time (b) normalized number of cells vs time.

If we follow the curves, starting with t_0= 0 h is the time when we took the first image (it was two hours after the radiation), the number of cells directly started to decrease and continued decreasing till t_1= 25 h. At time t_1, the number of cells started to increase till

t_2= 75 h, then it went down till the end. Thus the number of cells acts differently in three different time intervals, i.e., from t_0 to t_1, from t_1 to t_2, and finally, from t_2 to the end.

From t_0 to t_1, which is approximately one day, this interval represents the direct effect of the radiation on cells, which means that the cell started to die, and the number of cells decreased, so the death rate is much bigger than the proliferation rate. Then, from t_1 to t_2, the number of cell back increases, which indicates that some of the affected cells tried to recover from the radiation and tried to duplicate, which implies an increasing number of cells. We conclude that the proliferation rate is the dominant in this stage. Finally, even if the cells try to recover from the damage caused by the radiation, at some point, they cannot do this anymore. Hence, they die, which coincides with what we previously said about radiation's effect on cells.

Now, let us look closer at the different curves inside the plot of the normalized number of cells with time to visualize the effect of pH on this process. The plot presents the main differences between the curves.

Beginning with the t_0-t_1 time interval, the curve for pH=7.1 and pH=8.9, the growth rate decreases almost the same way. In other words, they have the same slope, but pH=6.2 has a lower slope, meaning the growth rate is greater here. Hence, when the cells are in an acidic medium, they can resist radiation. At this time, if we take the second interval, the growth rate starts to increase also, similarly for pH=8.9 and pH=7.1, but it appears that for pH=7.1 curve shows that the cells can repair itself that the curve pH=8.9, but one more time, the cells in pH=6.2 have a higher growth rate (higher slope). In conclusion, slightly acidic conditions allow the cells to maintain growth rates to produce more cancer cells and induce radiation resistance.

4.2 Cellular Automaton model

4.2.1 Introduction

Mathematical modeling is a tool used to represent and explain a real system by creating an artificial system whose properties can be adjusted to examine, analyze and predict the events in this system. Computational modeling or simulation helps to describe complex systems such as biological systems. The definition of a biological system is a complex network of biological entities (Collins Dictionary). However, developing a practical model for this kind of system requires a good background in both math and biology. In this work, we will talk in detail about how we build a model that describes the cell growth

of a type of brain tumor. In the past few years, many models were proposed to visualize the growth rate of untreated and treated gliomas by considering two significant biological phenomena at the cellular scale: proliferation and diffusion (56). The easiest way was to introduce the proliferation function (cell division) as a differential equation in time. This function could be represented by exponential proliferation, logistic law, or Gompertz law. On the other hand, the spreading of tumor cells in space (cell migration) was studied by assuming that the diffusion could be a random motion of cells. Finally, both the cell division (time component) and cell migration (space component) combined to get the proliferation-diffusion equation which will help to study the behavior of the cells (57-62), the variation of the cell concentration during a small dt, in a small slice of space between x and x+dx is represent: Proliferation + Diffusion.

Our project implemented a mathematical model using the agent-based method on a two-dimensional domain. Agent-based modeling (ABM) is a bottom-up simulation technique to study a complex system where the system is analyzed by its individual elements (agents) interacting with each other. These agents can be controlled using simple rules. The critical point of this model is the emergence of macro-level effects from micro-level actions and interactions (63, 64). In our model, the tumor cells are the agents that will be biased using conditions applied as inputs to study the overall outcome of our biological system. The model follows the proliferation-diffusion equation; a death term was added because this term came from using the radiotherapy technique to kill the cancer cell. This term was also introduced as a differential equation in time, so the equation became: Proliferation + Diffusion – Death.

In parallel with our experimental work, a mathematical model is built according to the results obtained from the experimental data. This model has studied the growth rate of the tumor cells combined with the proliferation and death terms.

4.2.2 Description

Briefly, this model is based on a cellular automaton, i.e., a model discrete in time and space, the space is a lattice, and each site can either be empty (filled with 0) or occupied (filled with any number) by at most one cell. The model is acquired by defining some parameters such as the area of space, the initial number of cells, the probability for cells to move, proliferation rate, death rate, and waiting times (the waiting times here refers to the times when the system feel an influence from the radiation i.e. t_0, t_1, and t_2).

First, the space is defined as a matrix, and the length of this matrix is (L). Then, the initial number of cells (N) in which these cells will be randomly placed inside the space to occupy some sites is also defined, and the number of the time step should be defined. The length of space, the initial number of cells, and the number of time steps are selected at the beginning to be small in order to check that the model is running properly. In the second step, probabilities of moving and proliferating were given to each cell. The probabilities were defined as arrays containing random numbers between 0 and 1, and each cell will have a value from each array. That values represent probabilities for the cell to move and proliferate. After this, the cells could move, proliferate, or do both. However, the cell's movement and proliferation occur under some conditions. The first one is the cells must have probabilities smaller than the probabilities that are given to the system. The second one is if at least one empty site surrounds the cell. If there is more than one empty place, the cell randomly chooses one of these empty sites. Now, what about the cells located on the border of the space?

The first implementation issue was dealing with the cells on the border if they needed to move or proliferate. Periodic boundary conditions are applied to the system to solve this issue, meaning that if the cell on the border moves out of the space, it will enter from the opposite side of the space.

Next, an example is used to explain what actually happens when the model is run. If the length of the space L=5 units, N= 10, the probability to move=0.3 and the proliferation probability=0.3. Cell (2) is selected to understand the model. If the movement probability of the cell is smaller than 0.3, cell (2) will move, if it is not, it will stay on the same site. If cell 2 moves, it will randomly choose one of the neighboring empty sites to move to it. Introducing the lattice at t= 0. Note that each cell will have 8 neighbors some of them empty or all of them are empty or all of them will be full.

Scheme 4.1

(a) *A lattice with 5 unit length, it has empty (filled with 0) site or occupied (filled randomly with any number from 1 to 10. (b) it is extracted from the image (a) to show the neighbors of cell (2)*

L

1	0	0	0	9
0	6	0	0	4
0	0	2	0	0
8	0	0	10	0
0	3	0	5	7

L

(b)

Cell (2) has two neighboring sites are filled and six are not. So, randomly will choose one of these six empty sites.

6	0	0
0	2	0
0	0	10

(a)

Then cell (2) can move to one of the empty sites, let's say it moved randomly to the right one, so it left its original site empty. Then, at the first time step (N_t=1), the lattice will be as this:

Scheme 4.2

The same lattice in scheme (4.1) but here the cell (2) changed its location (highlighted with yellow)

L

1	0	0	0	9
0	6	0	0	4
0	0	0	2	0
8	0	0	10	0
0	3	0	5	7

L

In the next time step (N_t =2), let's select a cell from the border to see how it worked for periodic boundary condition. Let's take cell (9), the neighbors for cell (9):

Scheme 4.3

It is extracted from the scheme (4.2) to show the neighbors of cell (9)

5	7	0
0	9	1
0	4	0

Cell (9) has four neighboring sites are filled and four are not. So, randomly will choose one of these four empty sites.

Scheme 4.4

The same lattice in scheme (4.2) but here the cell (9) changed its location (highlighted with green).

L

1	0	0	0	0
0	6	0	0	4
0	0	0	2	0
8	0	0	10	0
9	3	0	5	7

L

For proliferation, the same concept is used. The cell must have a proliferation probability smaller than 0.3 and has at least one empty site in order to give the new cell (that formed from the duplication). One thing that should be noticed is that the number of cells in each proliferation event increased by one. Let's take cell (6), which will proliferate at the third time step (N_t =3).

Scheme 4.5

It is extracted from the scheme (4.4) to show the neighbors of cell (6)

1	0	0
0	6	0
0	0	0

Cell (6) has one neighboring site is filled and seven are not. So, randomly will choose one of these seven empty sites

So, cell (6) will add a new cell to the system, in order to count it, it will has the name cell (11), and the lattice will be

Scheme 4.6

The same lattice in scheme (4.4) but here the cell (6) is proliferate to add a next cell (11) (the cells highlighted with purple).

L

1	0	11	0	0
0	6	0	0	4
0	0	0	2	0
8	0	0	10	0
9	3	0	5	7

L

This is an easy example to understand the model. However, we should note that in our model, in each time step, not only one cell will move or proliferate. Actually, in each time step, each cell has probabilities smaller than the probabilities to move or to proliferate will move or proliferate or move and proliferate at the same time, and in the next time step, the system may have more cells, and some cell's sites will change.

After enough time steps, the number of cells will increase until the cells occupy all the sites in the lattice, and the number of cells will stop growing at this time, meaning it reaches saturation. The following curve represents the relation between the number of cells (counts) and the time step for the system that has L=20 and moving probability = 0.3, and growth probability = 0.4.

Figure 4.2

Counts vs timesteps in the case "with no radiation"

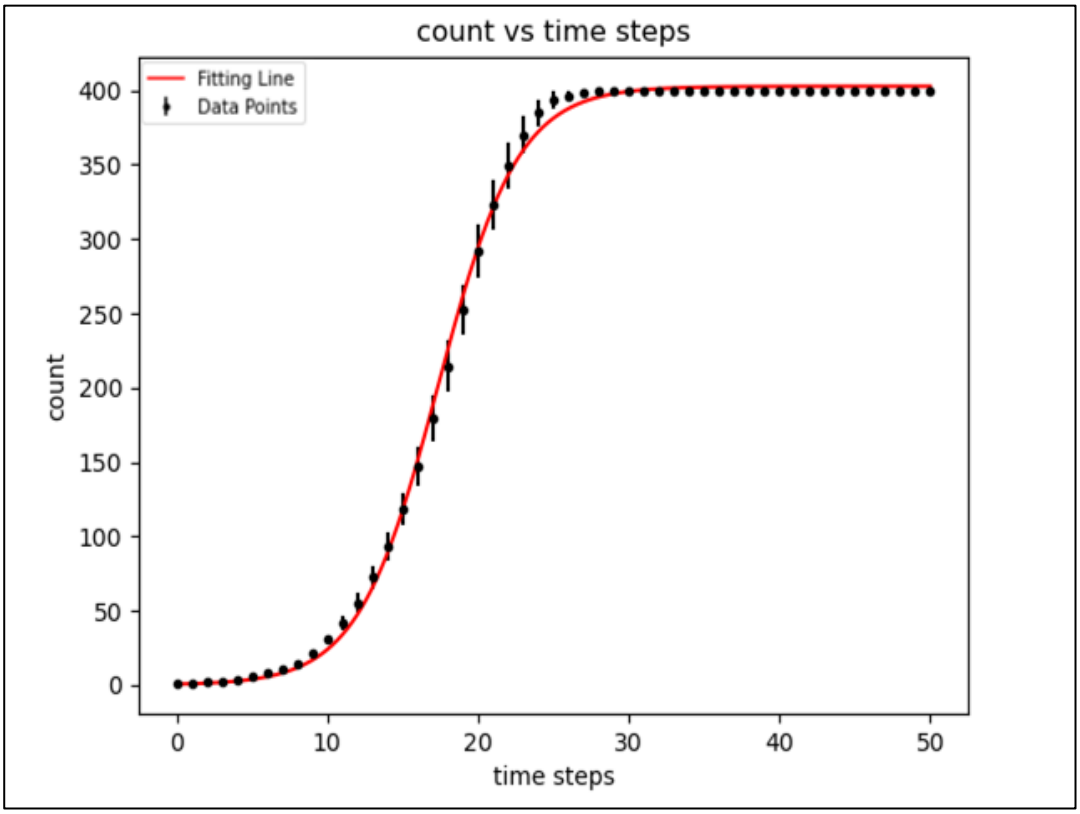

Here the plot in fig.(4.2) is fit using the logistic function with guessing initial values.

$$f(x) = \frac{a}{1+e^{-b(x-c)}} \tag{4.1}$$

The parameters got as following:

a=402.724

b=0.3762

c=17.354

(a) represents the maximum value of the function, and in the simulation, the maximum must be 400 since the system have only 400 sites in the space (20 x 20) matrix, but the fit

value is approximately 402. Maybe the fit value is not that good because, in real life, cells will never fill all the space if there are a lot of cells, the cells will start to die, so they will never fill the 400 sites. For (b), (b) represents the growth rate of the function, and in the simulation, the proliferation rate = 0.4, we can't compare these values directly, we need to follow this logic, if we started with initial number of cells (N_0) and the proliferation probability is (pp), the number of cells N after 1 iteration will be: $N = N_0 + N_0 \times pp$ so $N = N_0(1 + pp)$ Then after n iteration: $N = N_0(1 + pp)^n = N_0 e^{n \ln(1+pp)}$ where n is the time in iteration number. So we need to compare b with $\ln(1 + pp) = \ln(1 + 0.4) = 0.34$ which makes the two values close to each other. The last parameter is (c), (c) representing the value of the sigmoid midpoint. In general, the logistic function succeeded in describing the cell growth in the model.

Now, the death probability is added to the system in the same way. The cells were given a new probability, if the cell's probability was smaller than the death probability, then the cell would die. If the death term is added to the last example, for example, cell (8) will die, and hence, the site will be replaced by (0).

Scheme 4.7

(a) (b) are *the same lattice in scheme (4.6) but here the cell (8) it is disappeared and replaced with (0) (the cells highlighted with gray).*

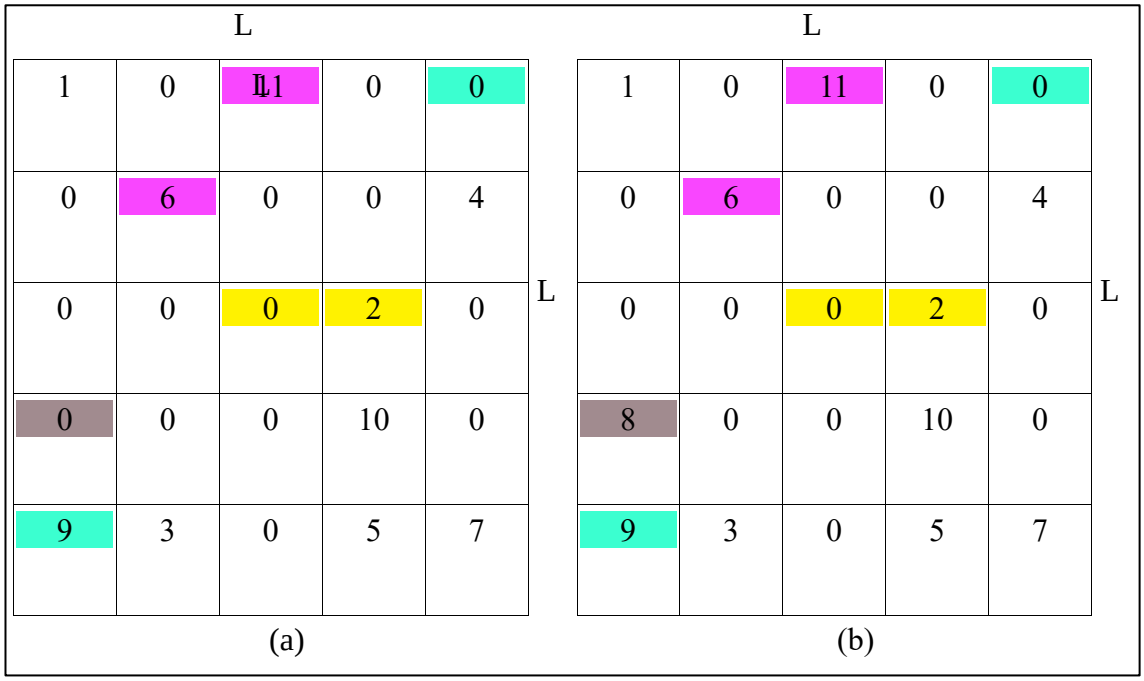

At this point, all the needed parameters were added to the system in order to study the cell growth with time and then to compare the results obtained from the simulation with our theoretical results. However, all the parameters should be adjusted.

4.2.2.1 Compare (Discussion) the experimental results with some Theoretical results

In this part, a detailed talk about how the model was modified in a way to fit our theoretical results. After adding the death probability to the system and making sure that the system is running correctly, the death probability should be adjusted to follow the trend of the theoretical curves, so the death term was added as a step function where its value changes with time, because as reported before the effect of radiation changed with time, at first there was a direct effect of radiation after a while this effect it was low because the cells tried to recover making the proliferation probability the dominant over the death probability in this interval, and then the delayed effect of radiation caused the death of the cells.

In the system of 20 x 20 space, the initial number of cells = 50, 50-time steps, movement probability = 0.3, proliferation probability = 0.3, and death probabilities 0.4 for t= [1, 15], 0 for t=] 15, 22[, and 0.5 for t= [22, 50], these parameters were chosen by hand in order to get the trend of the curve as in our experimental results.

Figure 4.3

Counts vs. time steps in the case "with radiation"

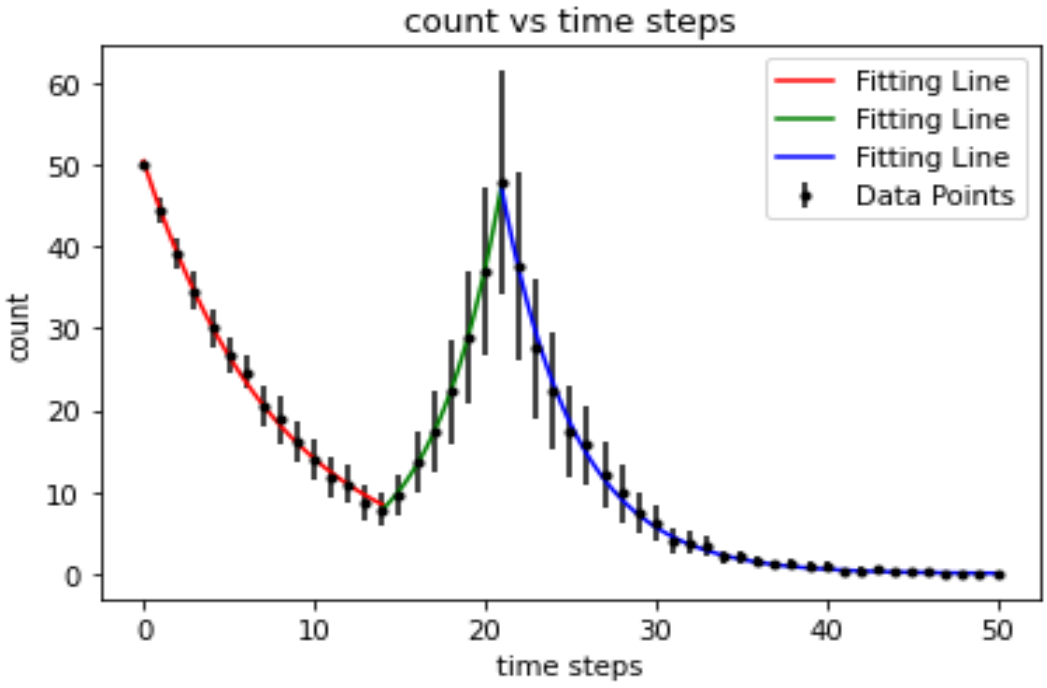

Fig. (4.3) represents the number of cells with time steps in a system containing cells that were moving and proliferating after this system was affected by radiation which induced the death of the cells.

The logistic function was used to fit the simulation data in different time intervals. Each interval represented by different color, following each fit has its fitting parameters.
In the interval (0-14) as represented by red color the exponential decay function was used here and the fitting parameters were as following:

$$f(x) = a_1 e^{-b_1 x} \tag{4.2}$$

a_1=50.36284887

b_1=0.12712133

Here the growth rate is 0.12 following the same logic as before but we add the death probability (dp), in this case, after n iteration: $= N_0(1 + pp - dp)^n = N_0 e^{n \ln(1+pp-dp)}$. So we need to compare b_1 with $\ln(1 + pp - dp) = \ln(1 + 0.3 - 0.4) = -0.11$, one more time the values close to each other and the minus sign for the deacreasing.
The interval (14-22) represented by green line was fitted using the logistic function

$$f(x) = \frac{a_2}{1+e^{-b_2(x-c_2)}} \tag{4.3}$$

And the parameters were as following:

a_2=6.67864197 x 10^2

b_2= 0.266915648

c_2= 30.6102301

Here b_2=0.27 compare it with $\ln(1 + pp) = \ln(1 + 0.3) = 0.26$ hence here no death probability.

Finally, in range (20-51), one more time the exponential decay function was used

$$f(x) = a_3 e^{-b_3 x} \tag{4.4}$$

a_3=6.38624520 x 10^3

b_3=-0.233961736

The growth rate =0.233, and $\ln(1 + pp - dp) = \ln(1 + 0.3 - 0.5) = -0.223$
So this fit worked well in this case.

Even though the fit works well and gives close results to the entered simulation data, there was a problem at the sharp points at timestep=14 and timestep=22, and this sharpness comes when the simulation parameters are applied for all cells at the same timestep, which means that all cells will start to recur at the same timestep = 14 or start to die at the same timestep=22 which is not the case in the real system, what happens actually, each cell will choose different timesteps to recur or to die, so, how this problem solved?!

There is a programming method in Python called object-oriented Programming (OOPs), which is a programming model that structures programs so that behaviors and properties are bundled into individual objects.

OOPs method starts by defining a class, and the class is defined as a set of instance variables that define a particular object type, and in our system, the class is a cell, and then an object is defined. The object represents a property that is given to the class. In this system, T_1 and T_2 were the objects used in our model, where T_1 represents a gaussian distribution array around the time step 15 in order to give each cell a specific T_1 value around or equal 15, and T_2 represents a gaussian distribution array around the time step 22 in order to give each cell a specific T_2 value around or equal 22. The challenge was for each new cell formed because of the proliferation needed to add new T_1 and T_2 values for this new cell. OOPs method helped in solving the sharp point's problem. Now, a new plot got for counts vs time steps.

Figure 4.4

Counts vs timesteps in the case "with radiation" after applying OOP's method

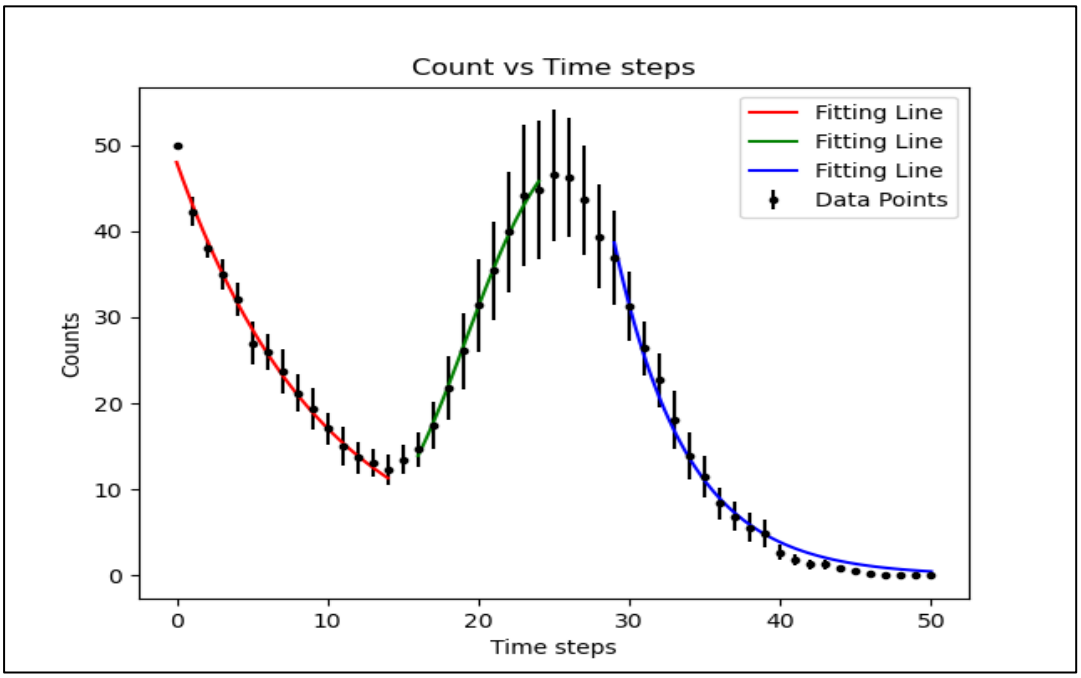

The fit of this plot is the same as before but with other parameter values
Red one with the exponential decay

$$f(x) = a_1 e^{-b_1 x} \tag{4.5}$$

a_1=48.01803744
b_1=0.10318147
Green one with the logistic function:

$$f(x) = \frac{a_2}{1+e^{-b_2(x-c_2)}} \tag{4.6}$$

a_2=54.58517944
b_2=0.34047968
c_2=19.14631878

Blue one with the exponential decay function:

$$f(x) = a_3 e^{-b_3 x} \tag{4.7}$$

a_3=1.6696667x10^4
b_3=0.20922778

After ensuring the simulation ran well, it was then used to study the experimental data mentioned in the previous section that studied cell proliferation with time. Fig.(4.5) below shows that the model was able to study the experimental results for cell proliferation in different pH solutions. In order to get this figure, the parameters were changed by hand by choosing the best values that make the simulation curves match the experimental ones. The death probability, T_1, and T_2 were the only parameters that have been changed. T_1 and T_2 were chosen according to the bottom and the top values for each curve, and the death probability was adjusted because this probability changes with time, so the death probability was represented as a step function. For the first time interval, the death probability was larger than the proliferation probability. In the second time interval, the death probability was smaller than the proliferation probability because the cells tried to recover from the radiation effect, but then the cells did not succeed in recovering, so the

effect of radiation went back to dominate on the proliferation rate. For each curve, there was a different step function. The other parameters, such as the movement and proliferation probabilities, were fixed for all the curves.

The death step function was different because for each curve, there was a different pH value which this pH value affected the death probability.

Fig.(4.5) shows a good matching between the simulation and the results, where The simulation can give the same data trend. Even that, the pH effect was implemented in this model with the death probability. However, there was a problem in fitting the last data where the fit that used in the previous results it is not working for the results in fig.(4.5) which is a problem needs to be solved. It should be noted that the space component that describes the migration of the cells inside the space still not implemented in this model.

Developing this practical model helps to give the needed information for future experiments on this type of cell, like the growth rate and the migration of cells within the tissues.

Figure 4.5

Implementing the simulation result with the real experimental results

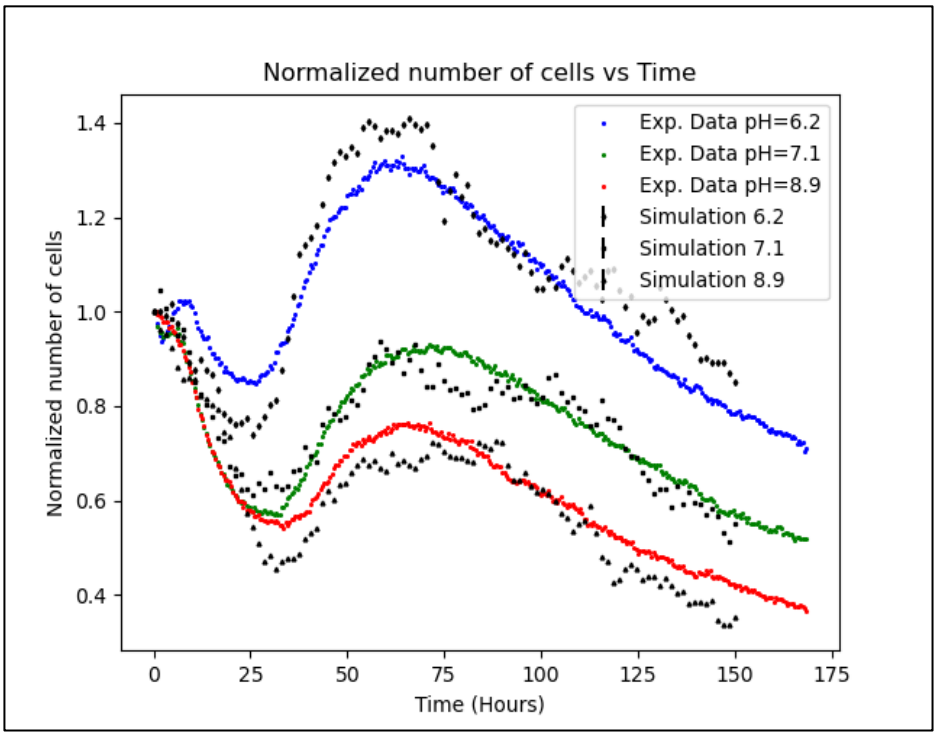

4.2.3 Cell Viability

In this section, we are concerned in studying the influence of the extracellular pH (pH_e) on radiation efficiency and then finding the optimal pHe of this treatment technique on the F98 cell line. Studying the cell viability of the cell population allows one to test the dual effect of radiation and pH_e modifications. Where the cell viability gives the number of viable (healthy) cells in a sample, it measures how efficient the treatment technique is against the specific cancer cell line. Hence, lower the percentage of cell viability, the more efficient the treatment technique is. Previous studies found that acidic pHe relieves immune response (65), so we expect that acidic pHe will increase the effect of radiation on the cell line.

In this context, we are going to use resazurin (7-Hydroxy-3H-phenoxazin-3-one 10-oxide) assay as an indicator of cell viability, and follow the methodology in section (3.8).

Data analysis:

After collecting the data for the experiment, the percentage of cell survival for each condition was measured by dividing the fluorescence intensity for the nonirradiated well by the fluorescence intensity for the irradiated one. In other words, if F0 indicates the fluorescence intensity of the nonirradiated well with a specific pH value and Fx is the fluorescence intensity of the irradiated cell with a specific dose (x) for the same pH value, then the percentage cell survival for the well with this pH value and irradiated by dose= x and x could be 0 Gy, 10 Gy, 20 Gy, and 30 Gy is measured according to this equation:

$$Percentage\ cell\ survival\ (\%) = \frac{Fx}{F0} \times 100\ \% \qquad (4.8)$$

After measuring the percentage of cell survival for each condition, the percentage of cell survival was plotted vs the pH values for different doses. It is also plotted with the doses for different pH values. Here 5, 6, 7, and 8 pH values appear on the plot for easier argumentation.

Fig.(4.6) shows the influence of radiation on cell viability, and at any pH value this effect is noticeable. For the percentage cell survival vs pH plot, the blue line generally represents the control cell culture where the cells did not expose to any radiation, assuming that the percentage cell survival is 100%. After radiation, as expected, there was a significant difference noted between control cultures without radiation and the cultures exposed to radiation. After radiation exposure, the percentage of cell survival decreased in the

culture. This percentage is dose-dependent, where the less radiation dose, the more healthy cells in the sample. In addition, this plot also showed that this effect is prominent at the acidic pHe values in both 10 Gy and 20 Gy. However, for 30 Gy, the line is almost flat, which means this dose is very high, kills most of the cells, and it is hard to give any information about the pHe impact.

The percentage of cell survival vs dose confirms the results obtained from the first plot. For 10 Gy and 20 Gy, the less pHe values, the more influential the used dose, and for the 30 Gy dose, the points become closer to give a comparable value of percentage cell survival. Looking at curve pH= 5 there is a 35% decrease in cell viability at 10 Gy and a 45% at 20 Gy which means that there is an obvious effect from the radiation on cell viability at low pH value when we increase the dose, which is not the case for the other curves (other pH values), where there is no a big difference on cell viability between the 10 and 20 Gy.

The results showed that the acidic pHe provides a good radiation efficiency, which agrees with the studies that reported that acidic pHe relieves immune response making the radiation more efficient. Even though the acidic pH_e values increase cell growth, as mentioned in the previous results, is shows the opposite here, the reason of this contrary, in the time-laps microscopy a different pH solutions were used and the protocol is different; or maybe cells can be still attached to the bottom of the dish while being dead.

Figure 4.6

Cell viability results

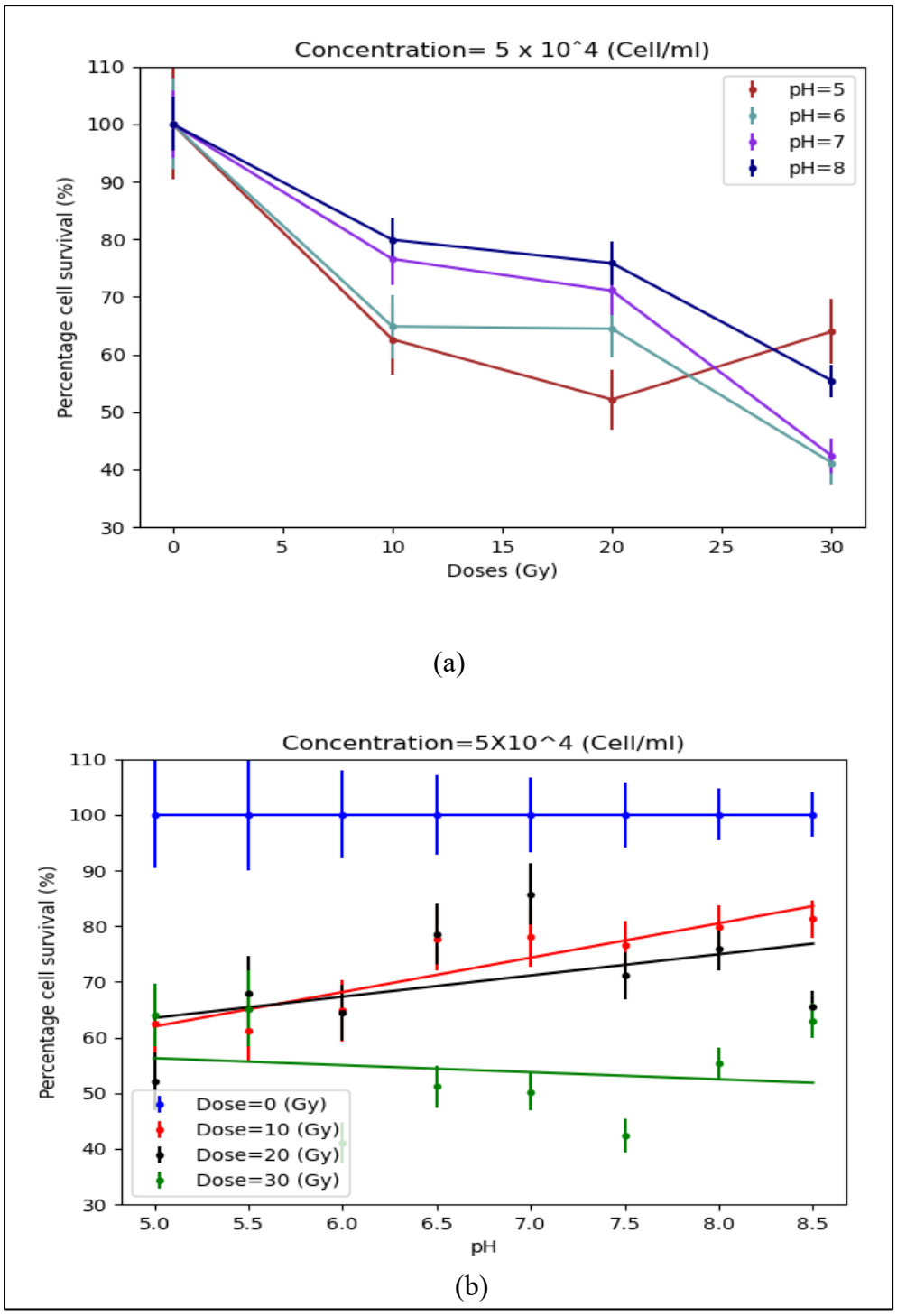

(a) Percentage cell survival vs pH (b) percentage cell survival vs doses. The results o btained 48 hour after radiation.

4.3 Measuring the intracellular pH (pHi) of the glioma F98-cell line

As mentioned above, the majority of tumor cells are associated with alkaline pH_i values of 7.1 to 7.6 and acidic pH_e values of 6.2 to 6.9, while normal cells originate with a lower pH_i (7.0–7.2) than that in the environment (7.3–7.4). These 'reversed' pH gradients influence cancer cell behaviors, including metastasis, proliferation, and metabolic adaptation. Consequently, it appears that measuring pH_i in tumors offers interest in observing the progression of cancers and the responses of cancer cells to various treatments (3).

A proper study of the evaluation of intracellular pH in glioma cells when they are affected by radiation and by altering the extracellular pH values will take place in this section. This experiment was performed using Carboxy SNARF- AM as a pH probe and by applying many imaging and measurement methods, such as the ratiometric pH measurement, i.e., ratiometric fluorescence is the technique where the intensities of two or more wavelengths of an emission or excitation spectrum are measured to identify changes to the local environment. However, the pH probe must be calibrated first and get the calibration curve. Following the protocol of the experiment in section (3.9)

Image processing and data analysis, you can see Fig. (C.1).

With our knowledge of the emission and excitation spectra for SNARF-1, the probe was excited using two wavelengths at 500 nm and 580 nm, and the fluorescence emission was recorded in the 550-640 nm range. Two images were taken for each well using the fluorescence microscope, one for the corresponding excited wavelength, to apply the ratiometric method to evaluate the internal pH.

Ratiometric fluorescence: The shifts between spectra obtained for acidic (protonated) and basic (deprotonated) forms of SNARF-1 can be exploited to carry out ratiometric measurements. In this case, pH is related to the ratio of the fluorescence intensities measured at two wavelengths, a feature of the indicator used. In our case, the ratio of the intensities was obtained when the intensities for two images were divided, and this was done by utilizing ImageJ/Fiji and Python as follows:

1- Convert the original image to a binary image (Masks) using Fiji. Nevertheless, the minimum threshold must be set to fit images of glioma cells. These binary images only

contain the relevant information of the cells with pixels set to 225 and background pixels set to 0, which helps to get only the pixels contributing to the intracellular signal. This is done automatically by running a macro written in java language.

2- After having the binary images, using Python, each image has been converted to a 2D array containing only the values 0 and 225. In this respect, all the indices of the 225 value were known. In other words, regions of interest were selected.

3- Then, the original images were converted to a 2D array containing the actual intensity in each pixel. The same regions of interest were selected in the original image using the information above.

4- Therefore, for original images of F98 cells, the 2D array of the 580 nm image was divided by the 2D array of the 500 nm image (pixel by pixel division) to obtain a new 2D array that holds values the intensity ratio for each pixel of the ratiometric image.

4.3.1 Calibration curve

Calibration means to determine, rectify, or adjust the graduations of something. In this context, the pH-dependent spectra of Carboxy SNARF-1 are remarkably different when the probe is loaded in cells, so calibration is a requirement for the F98 cell line. The nigericin method is the most widely used method to do the calibration (54) (66, 67). Adding nigericin and valinomycin to the solution allowed a rapid internal and external pH equilibration.

The presence of nigericin in a solution will create a proton/ potassium exchange at the cell membrane, so if the cells suspended in a solution contain potassium concentration close to the intracellular concentration of K^+ ions, this indicates that there will not be a net movement of potassium ions, in contrast, the hydrogen ions will move freely depending on their concentration gradient, therefore after a while, the concentration of hydrogen will be the same between inside and outside this means the internal pH will be set as the external pH. However, the intracellular potassium concentration is not precisely known, so adding an amount of valinomycin will help to get the equilibration of external and internal K^+ concentration, where valinomycin is very selective for K^+ over Na^+ within the cell membrane.

The equilibrium of the intracellular pH with the known extracellular pH solution and the knowledge that each pHi value corresponds to a fluorescence intensity ratio leads to a plot of the calibration curve: Ratio = f (pH_i). The calibration curve obtained is presented below.

Figure 4.7

Calibration curve

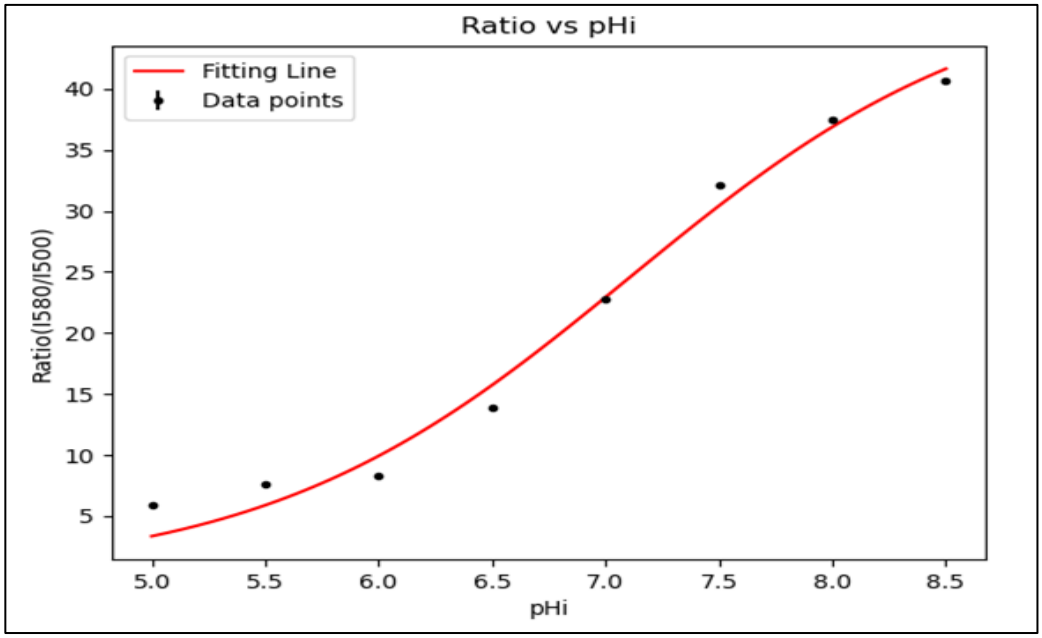

Calibration equation obtained by fitting the data

$$Ratio\ (pH_i) = \frac{48.895}{1+e^{-1.242(pH_i-7.012)}} \tag{4.9}$$

This turns the equation into

$$pH_i\ (Ratio) = \frac{-1}{1.242}\left[ln\left(\frac{48.895}{Ratio} - 1\right) - 8.826\right] \tag{4.10}$$

4.3.2 Intracellular pH measurements

In this part, we will discuss the changes in the intracellular pH of the F98 glioma cell line due to placing the cells in solutions with different pH values in the presence of radiation. Also, we will quantify pH_i distribution across a population of glioma cells. As reported in different studies that the main parameter responsible for pHi changes is related to the H^+ ions movement by the membrane transporters (68).

According to the equation established from the calibration curve and the measured values of fluorescence intensity ratio by using the methodology mentioned above to analyze the

images, we were able to get the pH_i value for each pixel in these images and introduce the results as a pH_i map that represent the pH_i distribution inside the cell population Fig(4.8). Besides this, the mean of pH_i values for the whole cell population was measured for each condition, table (4.1). From the results below, if we start looking at the data for the non-irradiated cells (Dose = 0 Gy), this data was displayed to study if there is an effect on pHi by changing the values of extracellular pH only, also to see if the F98 cells have the ability to regulate their pHi (the range between 7.3-7.6) under the pHe changes, It is evident from the results that for very low pHe the cells exhibits low values of pH_i and increasing pHe value shows an increase in pHi values, this implies that there is a notable effect from pHe on pH_i. It is not a sudden effect because the results were taken after at least 4 h of suspending the cells inside the pH solutions, so they had time to regulate their pH_i, but they did not. Even though we note that there is still an inversion of the pH gradient as documented in tumor cells. If we also focus on the pH_i map for the non-irradiated cells, in acidic pH_e, the pH_i values vary at a narrow range, and this range becomes more expansive when the cells are placed in the basic pH_e. For the irradiated cells, we see a significant drop in the pH_i values after exposing the cells to radiation, which indicates that the radiation influences the pH_i of the cells. This influence increases at the acidic pH_e, because if we compare between dose=10 Gy and dose =20 Gy, we see that for acidic pH_e and higher dose, the drop in pH_i is more prominent, but in the basic pH_e the effect on the pH_i in both doses, it almost the same. In the pH_i map for the radiated cells, the pH_i is very homogeneous at the intercellular level because the pH_i values were measured at a narrow range. These are an interesting results but they need to be confirmed by repeating the experiment multiple times.

Table (4.1)

The mean pH_i values (M) obtained over all the cell population

	pH_i		
pH_e	Dose = 0 Gy	Dose = 10 Gy	Dose = 20 Gy
5	6.35202 ± 0.000239	4.01117 ± 0.000190	3.8297 ± 0.0000804
5.5	6.7474 ± 0.000266	4.1346 ± 0.000296	4.07242 ± 0.000231
6	7.07521 ± 0.000322	4.2770 ± 0.000172	4.18007 ± 0.000431
6.5	7.3720 ± 0.000454	4.3953 ± 0.000224	4.4897 ± 0.000210
7	7.7587 ± 0.000487	4.5027 ± 0.000221	4.59032 ± 0.000196
7.5	7.9441 ± 0.000871	4.6347 ± 0.000270	4.6678 ± 0.000139
8	8.1081 ± 0.000917	4.5937 ± 0.000195	4.64575 ± 0.000138
8.5	8.2599 ± 0.000827	4.6508 ± 0.000175	4.6974 ± 0.000168

Figure 4.8

pHi distributions in F98 cells at different radiation doses and different pH_e values

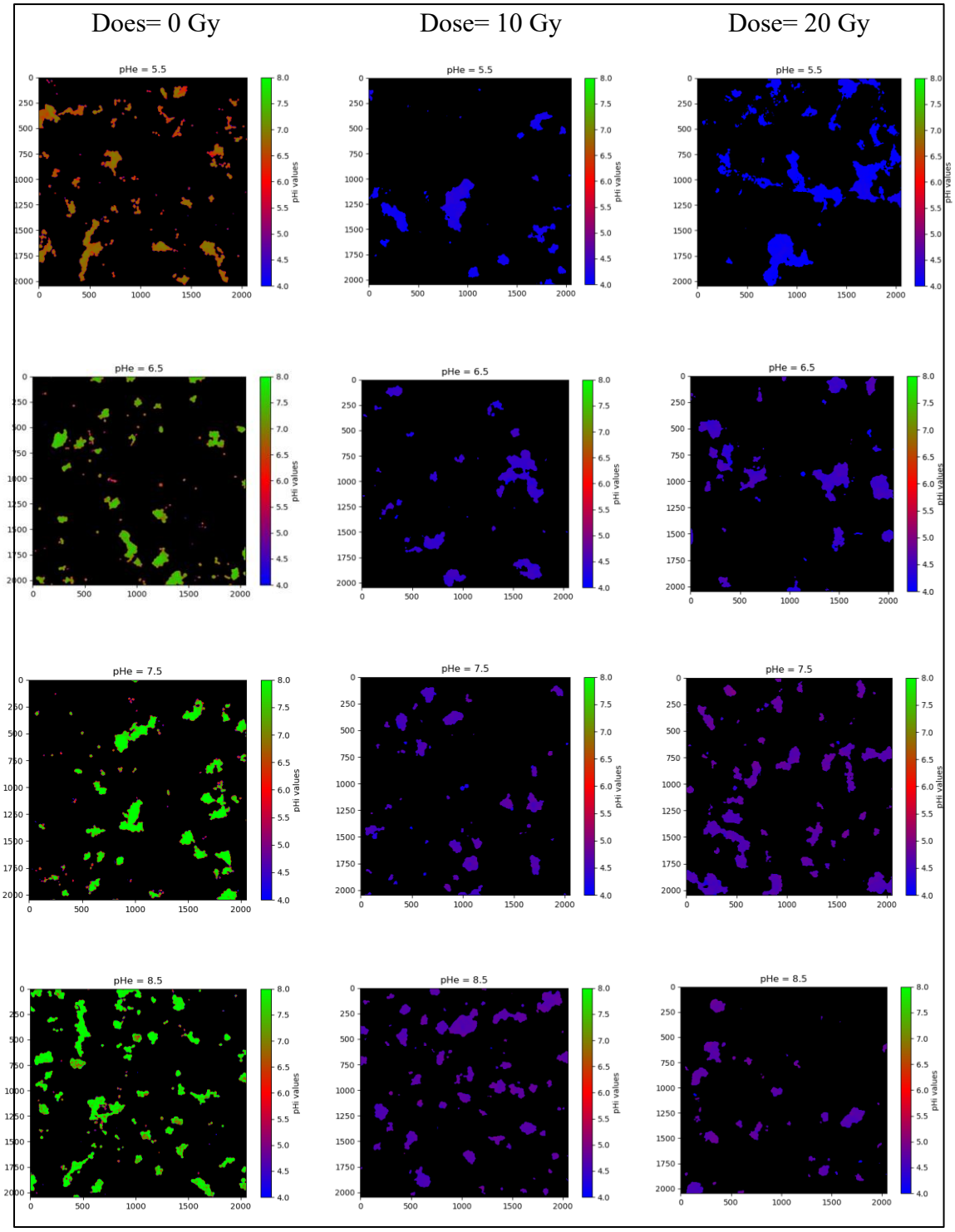

4.4 Conclusion and Perspectives

Believing that radiation will be this therapeutic technique that is highly pH-dependent since the Acidity of tumor microenvironment in cancer biology is becoming essential for clinical treatment, which gives the researcher a new hot topic based on studying this dependency between radiation and pH. So, this thesis sheds light on studying the joint effect between radiation and the regulation of both intracellular and extracellular pH of glioma cells using fluorescence microscopy. Therefore, the effect of radiation on the utilized cell line F98 organized in 2D by alternating the extracellular pH (pHe) was studied via two experiments. The first one used time-lapse microscopy, and the second one by measuring the cell viability, but the results of the two experiments were not consistent. One of the reasons for this contrary is that the protocols of the two experiments are different since two different solutions were used to alter the pH values, another limitation is that there was no time to repeat the experiments using the same pH solution because the time-laps experiment needs a long time, and the microscope is not available all time. Despite the contrary results of this part, they have hypothesized that manipulating the pHe will result in predictable changes in the radiation efficiency, which gives an argument for considering pH as a therapeutic target for future research based on the summation of radiotherapy with pH-regulating agents.

In parallel with the experimental part, a simple model was developed based on a cellular automaton that followed the proliferation of the cells organized in two dimensions before and after radiation and then tried to compare these theoretical results with the experimental ones. The model was successfully described cell growth before radiation, where the cells kept proliferating until they occupied the whole space and reached saturation; in this case, the proliferation represented by logistic law, which gave agreement with previous studies otherwise, adding the death term to this model and trying to change the parameters (probability to proliferate, the probability of dying, waiting times, etc.) in order to give the best match with the experimental results the results, in this case, were good, then the pH effects added inside the death probability to implement the model results with the cell proliferation results and as reported before the simulation results gave the same data trend as the experimental results, but this model needs more work, such as adding the migration of the cells inside the space.

The last part of this thesis was focused on studying the radiation's impact on the intracellular pH (pHi). In this part, a new technique was developed to apply ratiometric measurements for pHi via joining ImageJ with Python, and this technique may be more accurate than using ImageJ alone. The results of this experiment demonstrated that there was a significant drop in the pHi after exposing the cells to radiation; this gives an argument for considering the changes in pHi due to the radiation as a new biological effect of radiation on the cancer cell because it induces the death of the cells by lowering their intracellular pH, these results were very interesting, but still, they need to be approved.

List of Abbreviations

Abbreviation	Meaning
ATP	Adenosine triphosphate
ABM	Agent-based modeling
CSF	Cerebrospinal Fluid
DSB	Double-strand break
pHe	Extracellular pH
FADH2	Flavin adenine dinucleotide
pHi	Intracellular pH
IP	Ion pair
LINACS	Linear Accelerators
LET	Linear Energy Transfer
MLC	Multileaf Collimator
NADH	Nicotinamide adenine dinucleotide
OOPs	Object-Oriented Programming
OXPHOS	Oxidative phosphorylation
SSB	Single-strand break
SI	Specific ionization
WHO	World Health Organization

References

1. Lewanski CR GW. Radiotherapy and cellular signaling. Lancet Oncol. 2001.

2. Zhang X LY, Gillies RJ. Tumor pH and its measurement. J Nucl Med 2010.

3. Webb B, Chimenti, M., Jacobson, M. et al. Dysregulated pH: a perfect storm for cancer progression. Nat Rev Cancer 11. 2011.

4. Persi E, Duran-Frigola, M., Damaghi, M. et al. Systems analysis of intracellular pH vulnerabilities for cancer therapy. Nat Commun 9. 2018.

5. https://www.expii.com/t/nuclear-stability-definition-overview-8756.

6 .https://chem.libretexts.org/Bookshelves/General_Chemistry/Book%3A_ChemPRIME_(Moore_et_al.)/19%3A_Nuclear_Chemistry/19.08%3A_Nuclear_Stability#:~:text=For%20low%20atomic%20numbers%20most,neutron%2Fproton%20ratio%20is%201.518.

7. Victor M. Tello M, DABR. . Medical Linear Accelerators and how they work.

8. Saeed S. Dynamic Log Files Analysis For Diff 'rent Dose Rate IMRT event Dose Rate IMRT Using DVH and Gamma Index. 2015.

9. Nikjoo H, Uehara, S., & Emfietzoglou, D. . Interaction of radiation with matter. CRC press. 2012.

10. Attix FH. Introduction to radiological physics and radiation dosimetry. John Wiley & Sons. 2008.

11. Johns HE, & Cunningham, J. R. . The physics of radiology. 1983.

12. Baskar R, Dai, J., Wenlong, N., Yeo, R., Yeoh, K. W. . Biological response of cancer cells to radiation treatment. Frontiers in molecular biosciences, . 2014.

13. Targeted Therapy to Treat Cancer was originally published by the National Cancer Institute.

14. The French regulatory authority for Nuclear and radiation safety. 2006.

15. Radiation Therapy to Treat Cancer. National Cancer Institute website. 2021.

16. Haber AH, & Rothstein, B. E. . Radiosensitivity and rate of cell division:" Law of Bergonie and Tribondeau.". Science. 1969.

17. Yashar CM. Basic principles in gynecologic radiotherapy. In Clinical Gynecologic Oncology. 2012.

18. Brahme A. Comprehensive biomedical physics. Newnes. 2014.

19. Sharda N, Yang, C. R., Kinsella, T., & Boothman, D. . Radiation resistance. 2002.

20. Balagamwala EH, Chao, S. T., & Suh, J. H. Principles of radiobiology of stereotactic radiosurgery and clinical applications in the central nervous system. . Technology in cancer research & treatment. 2012.

21. Pouget JP. Basics of radiobiology. DNA repair. 2022.

22. Mladenov E MS, Soni A, Iliakis G. DNA double-strand break repair as determinant of cellular radiosensitivity to killing and target in radiation therapy. . Front Oncol. 2013.

23. Cannan WJ PD. Pederson DS. Mechanisms and Consequences of Double-Strand DNA Break Formation in Chromatin. . J Cell Physiol 2016.

24. Chmiel E MA. Fractionation (radiation therapy). 2021.

25. Mothersill C, & Seymour, C. B. . Cell-cell contact during gamma irradiation is not required to induce a bystander effect in normal human keratinocytes: evidence for release during irradiation of a signal controlling survival into the medium. Radiation research. 1998.

26. Gatenby R.A. GRJ. Why do cancers have high aerobic glycolysis? . Nat Rev Cancer. 2004.

27. Justus C.R. DL, Yang L.V. . Acidic tumor microenvironment and pH-sensing G protein-coupled receptors. Front Physiol 2013.

28. Anderson NM SM. The tumor microenvironment. 2020.

29. Koppenol WH, Patricia L. Bounds, and Chi V. Dang “Otto Warburg’s contributtons to current concepts of cancer metabolism". 2011.

30. Warburg O. "On the Origin of Cancer Cells." 1956.

31. Hanahan D. WRA. Hallmarks of cancer: the next generation. . 2011.

32. Vaupel P, Flood, A. B., & Swartz, H. M. Oxygenation status of malignant tumors vs. normal tissues: critical evaluation and updated data source based on direct measurements with pO2 microsensors. . Applied Magnetic Resonance. 2021.

33. Lagadic-Gossmann D, Huc, L., and Lecureur, V. . Alterations of intracellular pH homeostasis in apoptosis: origins and roles. Cell Death Differ. 2004.

34. Ward C, et al. "The impact of tumor pH on cancer progression: strategies for clinical intervention." In: Exploration of Targeted Anti-tumor Therapy 2020.

35. Bradley AJ, Lim, Y. Y., and Singh, F. M. . Imaging features, follow-up, and management of incidentally detected renal lesions. . ClinRadiol 2011.

36. Boedtkjer1 E PS. The Acidic Tumor Microenvironment as a Driver of Cancer. Annu Rev Physiol 2020.

37. Moolenaar WH, Defize, L. H., and de Laat, S. W. . Ionic signaling by growth factor receptors. J Exp Biol 1986.

38. Adenis AP, S.; Grammaticos, B.; Pallud ,J; Badoual, M. . Radiotherapy effects for diffuse low-grade gliomas. . 2021.

39. P.; Ellison D.W . LDNPARGVDAF-BDCWKOHWODK. The 2016 World Health Organization classification of tumors of the central nervous system: A summary. Acta Neuropathol. 2016.

40. Schneider T MC, Scherlach C, Skalej M, Firsching R. Gliomas in adults. 2010.

41. Barth RF, Kaur, B. Rat brain tumor models in experimental neuro-oncology: the C6, 9L, T9, RG2, F98, BT4C, RT-2, and CNS-1 gliomas. J Neurooncol 2009.

42. Lenting K VR, Ter Laan M, Wesseling P, Leenders W. Glioma: experimental models and reality. . Acta Neuropathol 2017.

43. Countess II FL automated cell counter User Guide (Pub.No. MAN0010644 E.0).

44. Stokes GG. "On the change of refrangibility of light,". Philosophical Transactions of the Royal Society of London. 1852.

45. Photophysics of fluorescent proteins iIdBS, France, .

46. Albani JR. Principles and Applications of Fluorescence Spectroscopy. Wiley-Blackwell. 2007.

47. Renz M. Fluorescence microscopy-a historical and technical perspective. 2013.

48. Minsky M. "Memoir on inventing the confocal scanning microscope". Scanning. 1988.

49. https://imb.uq.edu.au/files/52494/Confocal_Microscope_Diagram.png.

50. Żurawik TM, Pomorski, A., Belczyk-Ciesielska, A., Goch, G., Niedźwiedzka, K., Kucharczyk, R., ... & Bal, W. . Revisiting mitochondrial pH with an improved algorithm for calibration of the ratiometric 5 (6)-carboxy-SNARF-1 probe reveals anticooperative reaction with H+ ions and warrants further studies of organellar pH. . 2016.

51.https://www.thermofisher.com/documentconnect/documentconnect.html?url=https://assets.thermofisher.com/TFS-Assets%2FLSG%2Fmanuals%2Fmp01270.pdf.

52. Cafferty K. Application of Bayesian and Geostatistical Modeling to the Environmental Monitoring of Cs-137 at the Idaho National Laboratory. 2010.

53. http://www.gammaservice.co.uk/pdf/Gamma-GSRD1-Datasheet.pdf

54. Seksek Oea. “SNARF-1 as an intracellular pH indicator in laser microspectrofluorometry: A critical assessment”. In: Analytical Biochemistry 1991.

55. Hongu T, & Oskarsson, T. . Addicted to acidic microenvironment. Developmental Cell. 2020.

56. Powathil G KM, Sivaloganathan S, Oza A and Milosevic M. Mathematical modeling of brain tumors: effects of radiotherapy and chemotherapy. 2007.

57. Jbabdi S, Mandonnet, E., Duffau, H., Capelle, L., Swanson, K.R., Pélégrini-Issac, M., Guillevin, R. and Benali, H. . Simulation of anisotropic growth of low-grade gliomas using diffusion tensor imaging. Magn Reson Med. 2005.

58. Marusic M BZ, Freyer JP, Vuk-Palovic S. Analysis of growth of multicellular tumour spheroids by mathematical models. . 1994.

59. KR. S. Mathematical modeling of the growth and control of tumors. Ph.D. thesis, University of Washington, . 1999.

60. Woodward DE CJ, Tracqui P, Cruywagen GC, Murray JD, Alvord EC Jr. . A mathematical model of glioma growth: the effect of extent of surgical resection. 1996.

61. Tracqui P CG, Woodward DE, Bartoo GT, Murray JD, Alvord EC Jr. . A mathematical model of glioma growth: the effect of chemotherapy on spatio-temporal growth. . 1995.

62. Swanson KR BC, Murray JD, Alvord EC Jr. . Virtual and real brain tumors: using mathematical modeling to quantify glioma growth and invasion. J Neurol Sci 2003.

63. Luke DA SK. Systems science methods in public health: dynamics, networks, and agents. Annu Rev Public Health. 2012.

64. AT Crooks AH. Agent-based models of geographical systems. Springer Science+Business Media BV. 2012.

65. Lardner A. The effects of extracellular pH on immune function. J LeukocBiol. 2001.

66. Thomas JAea. “Intracellular pH measurements in Ehrlich ascites tumor cells utilizing spectroscopic probes generated in situ”. . In: Biochemistry 1979.

67. Seksek OaJB. “Nuclear pH gradient in mammalian cells revealed by laser microspectrofluorimetry”. In: Journal of Cell Science 109. 1996.

68. Doyen Dea. “Intracellular pH Control by Membrane Transport in Mammalian Cells. Insights Into the Selective Advantages of Functional Redundancy”. . In: Frontiers in Molecular Biosciences 9. 2022.

Appendices

Appendix A

Figures Supports the Thesis

Figure A.1

The Chart of the Nuclides.[5]

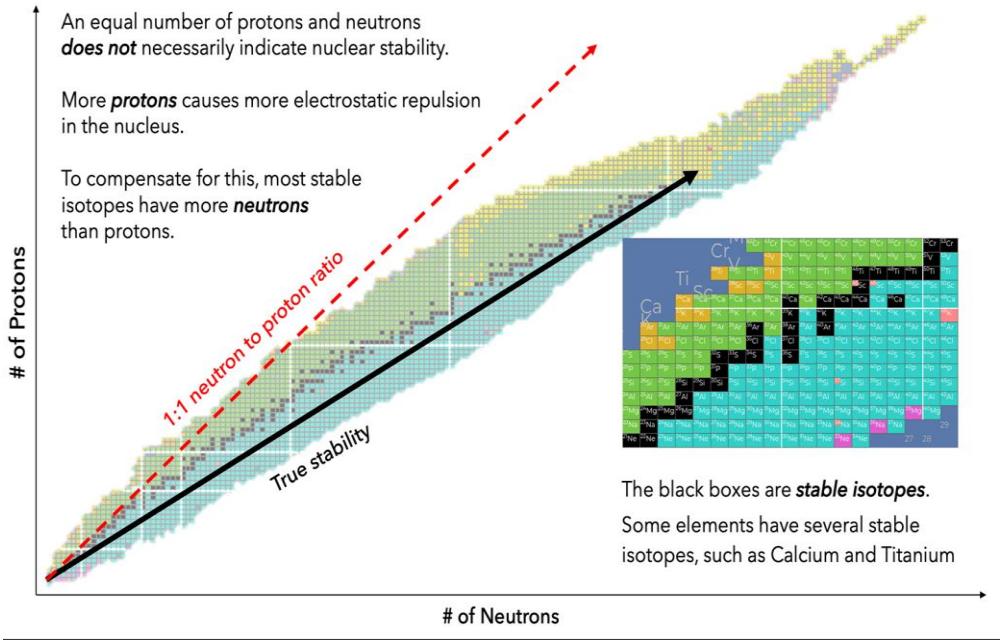

The following figure shows the main component of the linear accelerator

Figure A.2

The main components of (Linear) particle accelerator.

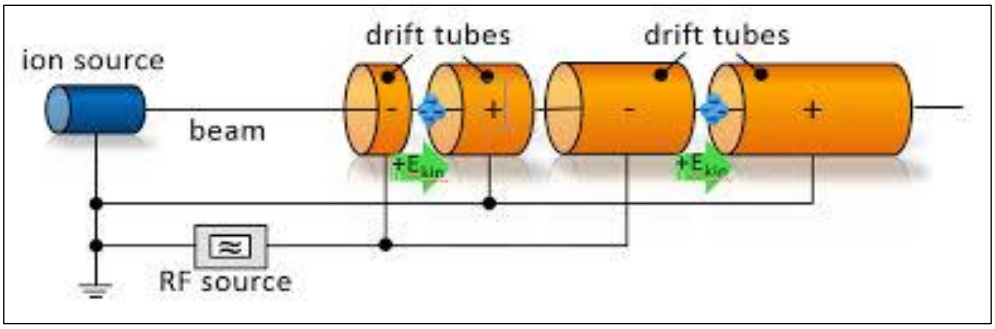

Figure A.3

The schematic diagram of a linear accelerator.

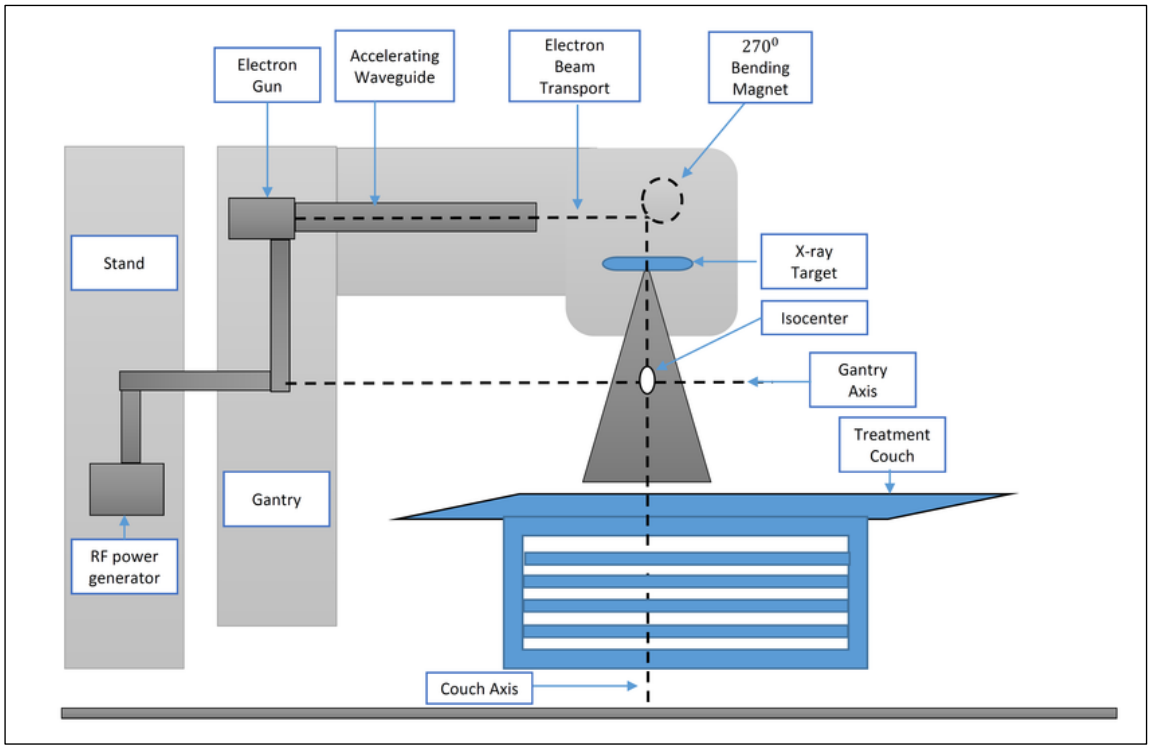

Figure A.4

Cell cycle diagram.

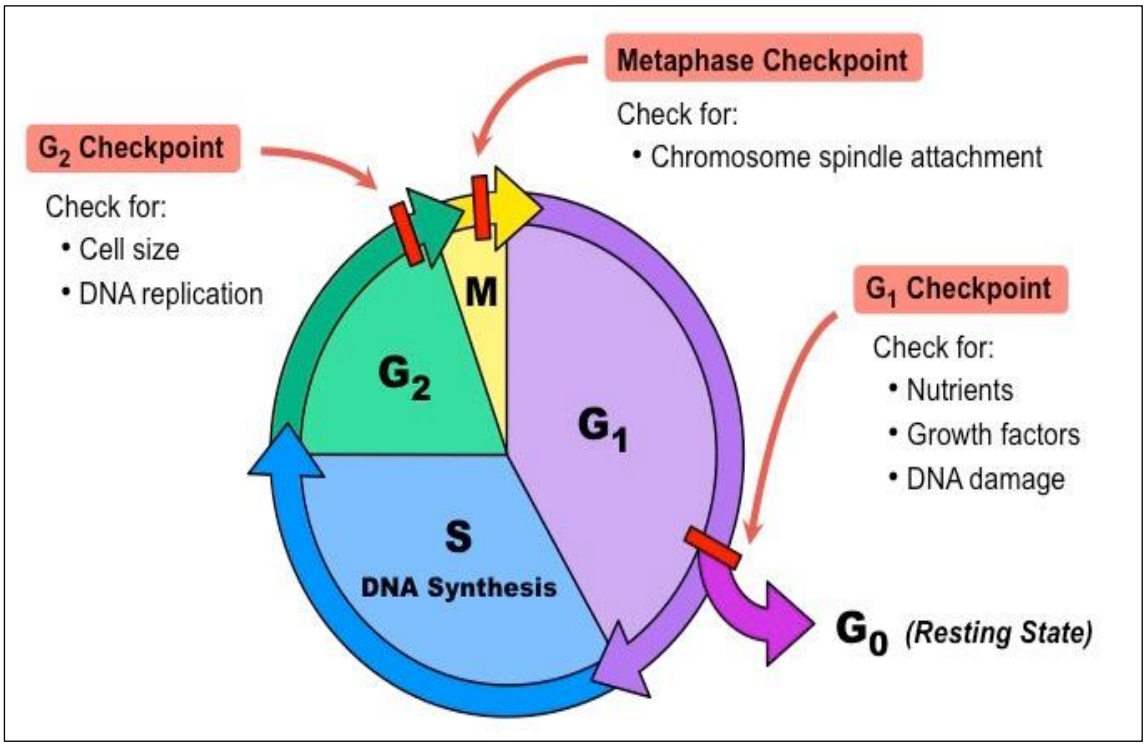

Figure A.5

The direct and the indirect effect of radiation on the cancer cells.

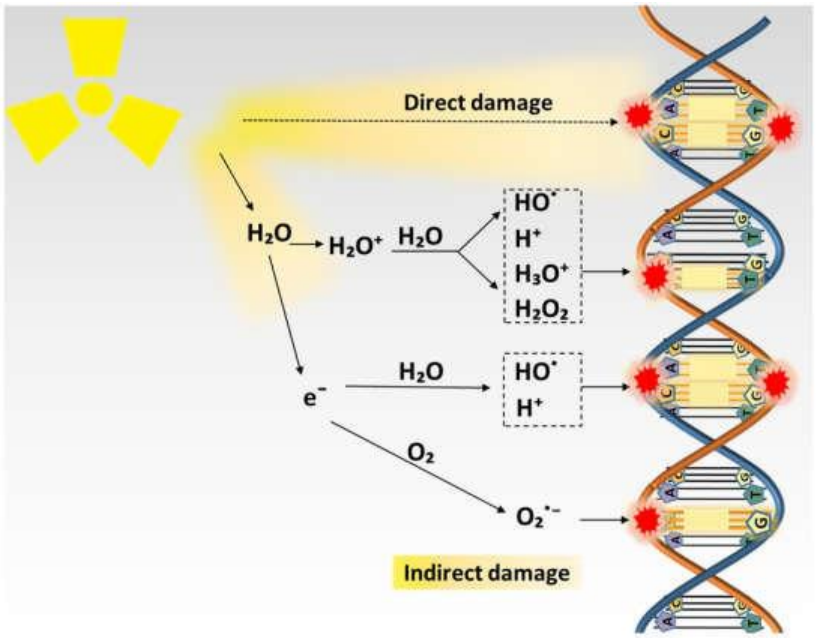

Figure A.6

hematic representation of anaerobic glycolysis (fermentation) and oxidative phosphorylations (OXPHOS) or mitochondrial respiration.

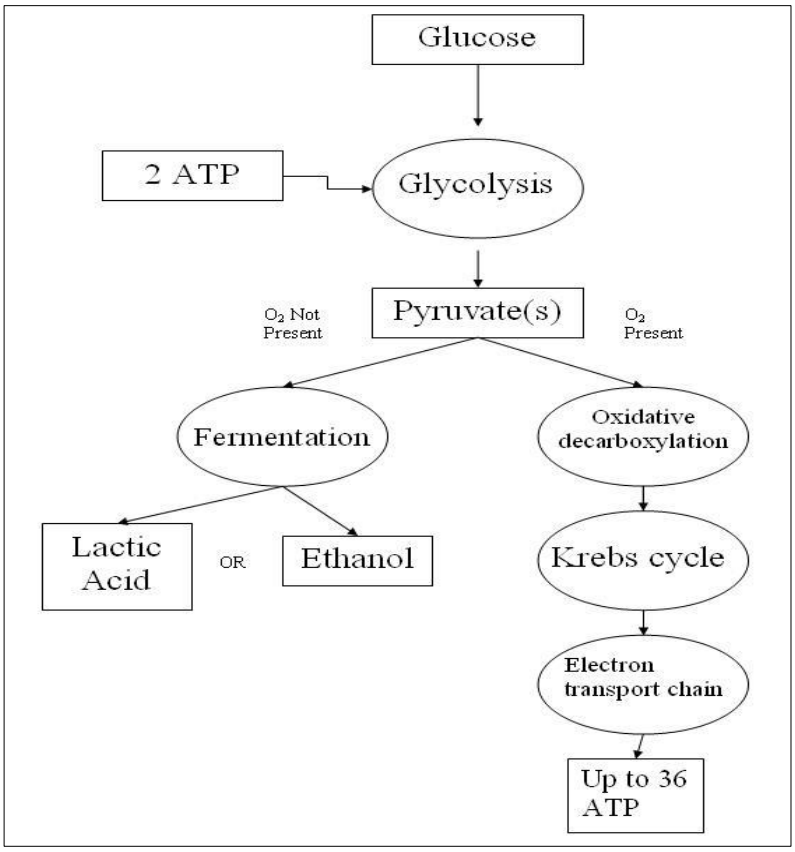

Figure A.7

MRI image for glioma.

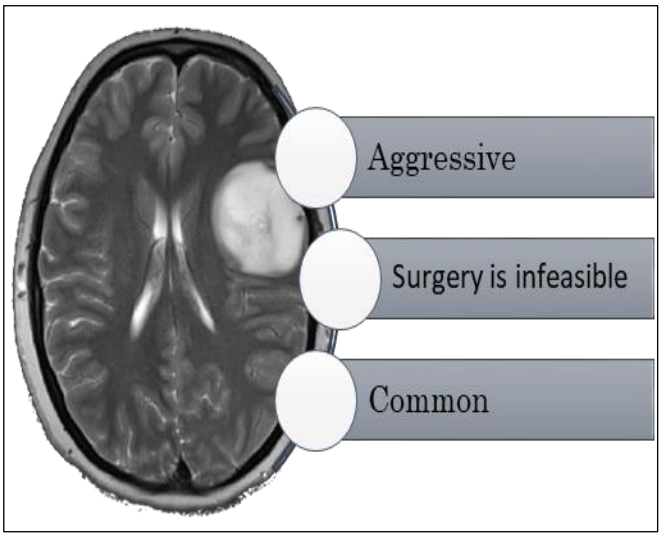

Figure A.8

Jablonski diagram.[45].

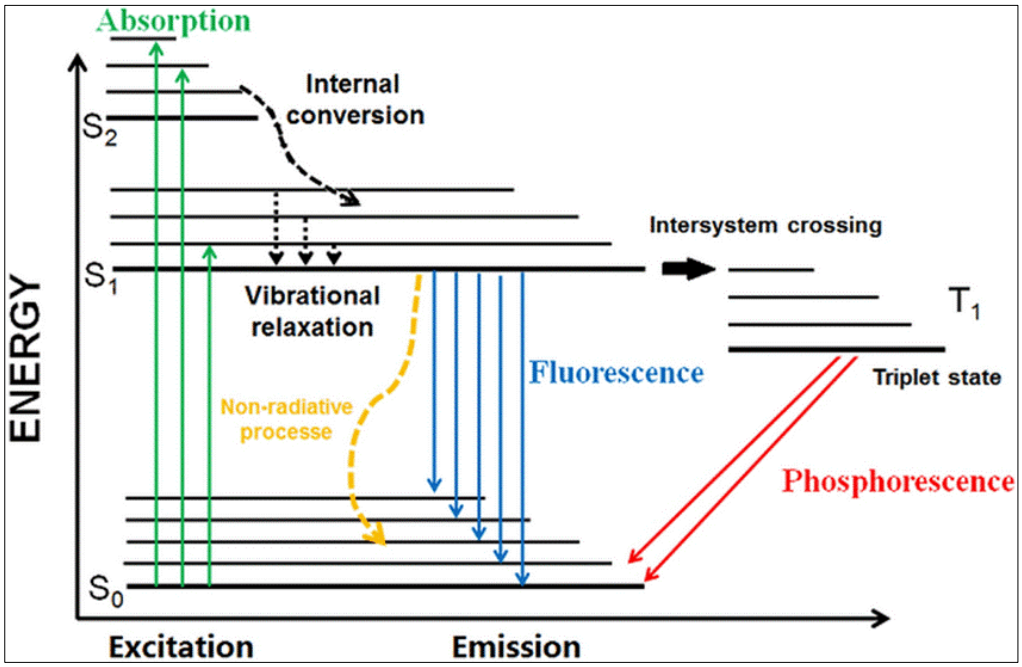

Figure A.9

Scheme of a confocal microscope. [49]

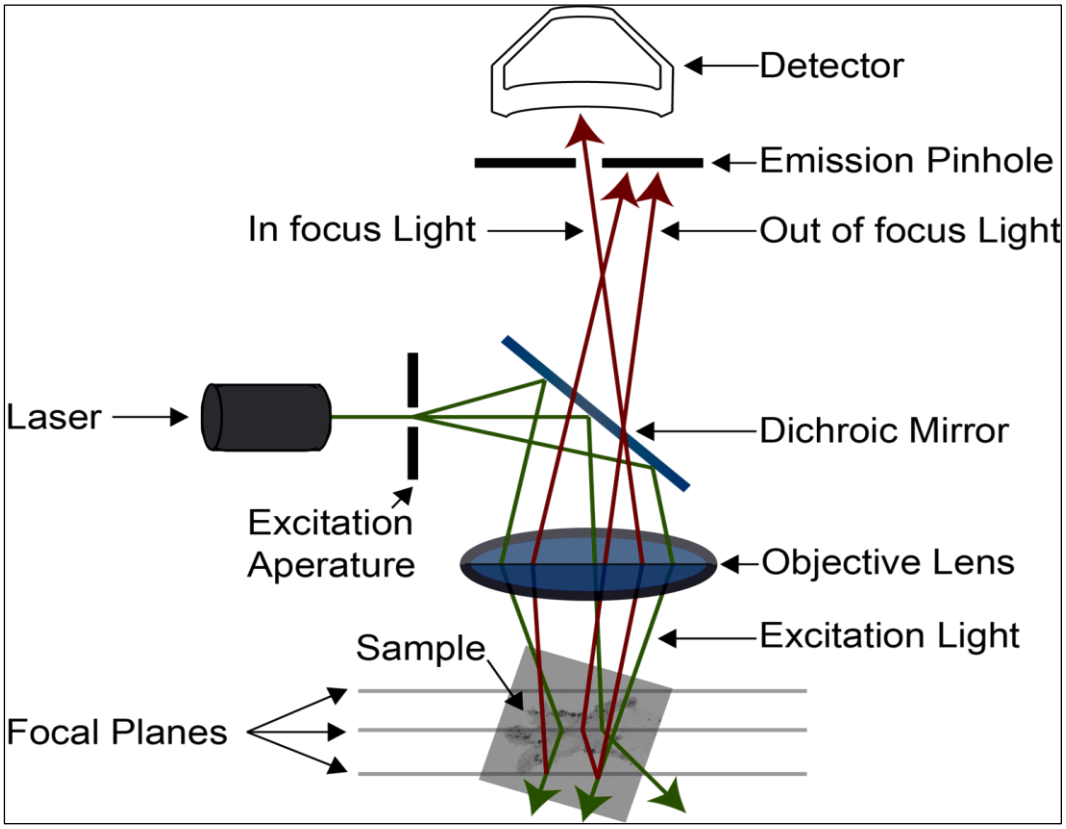

Figure A.10

(a) 2. Emission spectra of carboxy SNARF-1 in buffers at various pH values. Samples were excited at 488 nm. (b) Absorption spectra of carboxy SNARF-1.

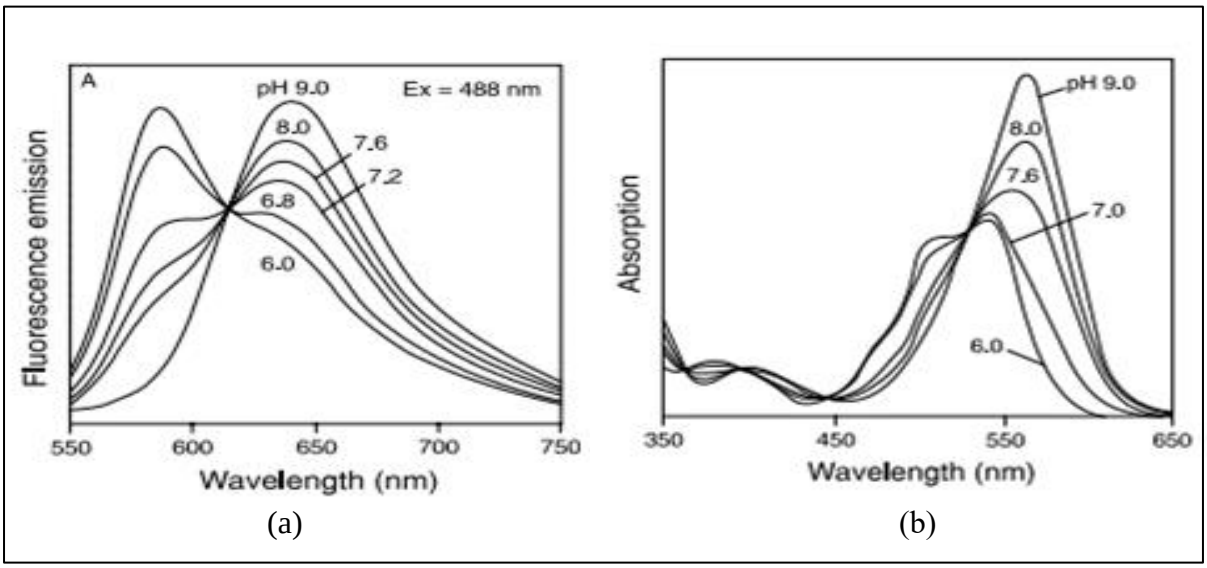

Figure A.11

Radioactive decay of Cs-137.

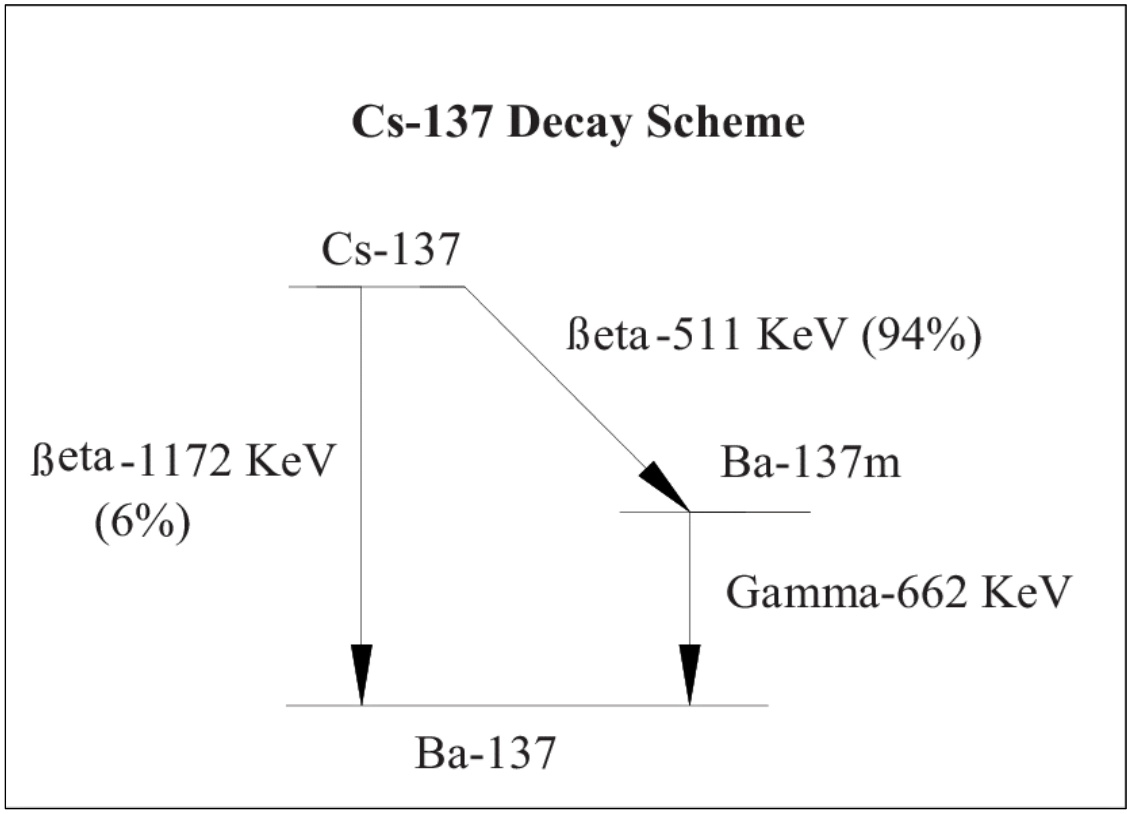

Appendix B

Figures for the materials and experiment Setup

Figure B.1

The incubator where we kept the cells for the experiments.

Figure B.2

Confocal microscope equipped with a camera and cellsens software, this setup used in the cell proliferation experiment and measuring the pHi experiment.

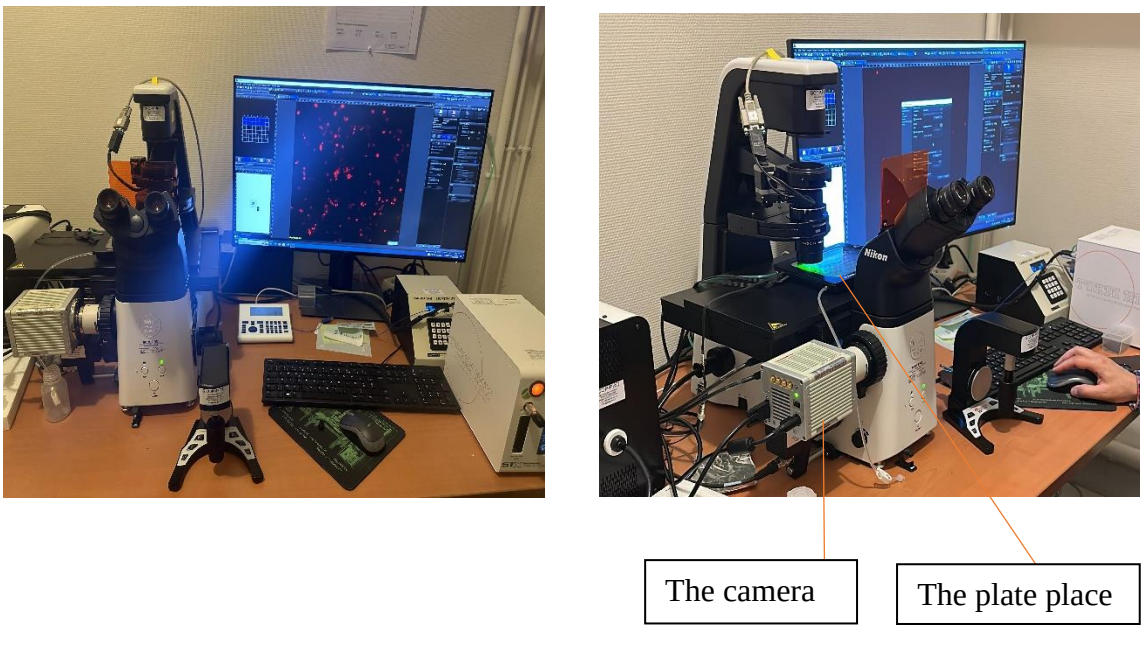

Figure B.3

Microplate reader that used in cell viability experiment.

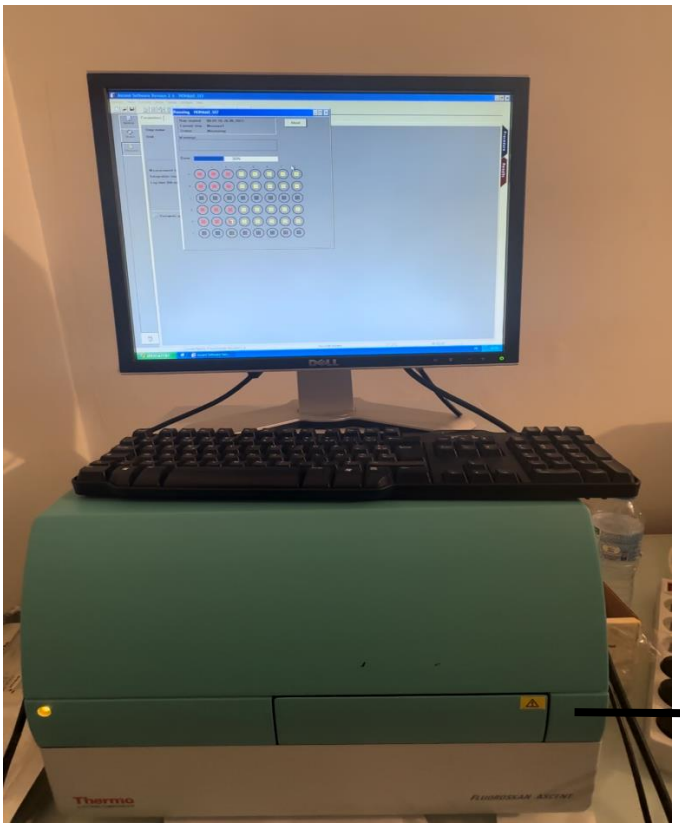

Figure B.4

The GSR D1 Gamma Irradiator

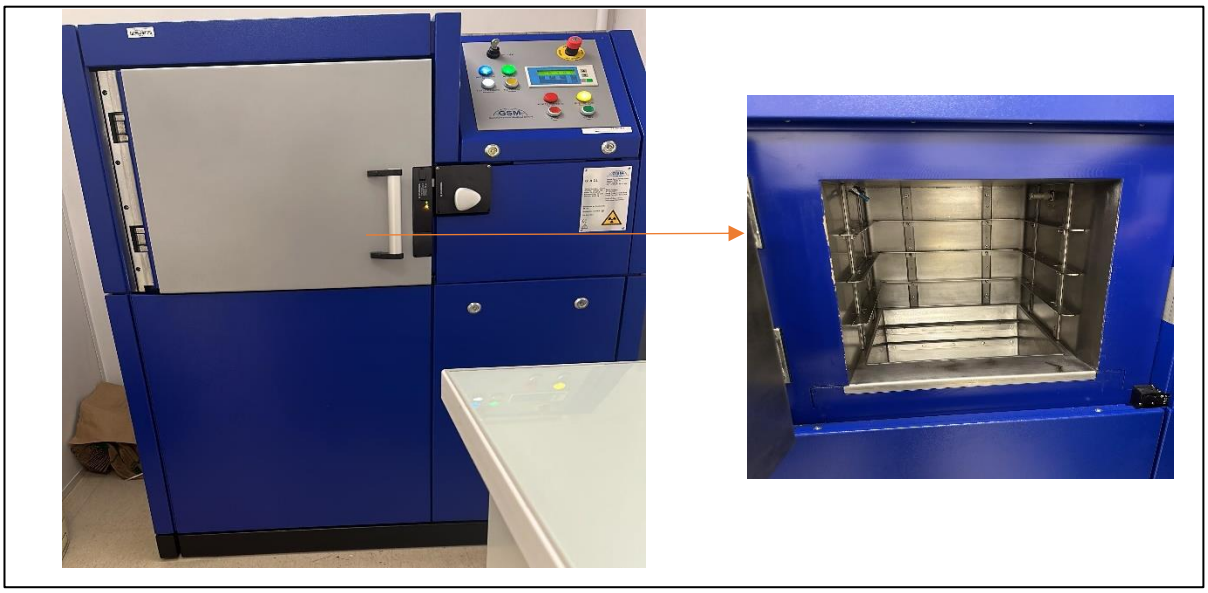

Appendix C

Figures for the data analysis for measuring pHi for the cell line

Figure C.1

(a)(b) Images for the cells placed in pH=5.5, with no radiation, (a) has been taken using excitation wavelength=580nm, (b)has been taken using excitation wavelength=500nm.(c) is the binary image of the image (a) were it contains only two values 0 for the background and 225 for the cells.(d) is the binary image of the image (b).

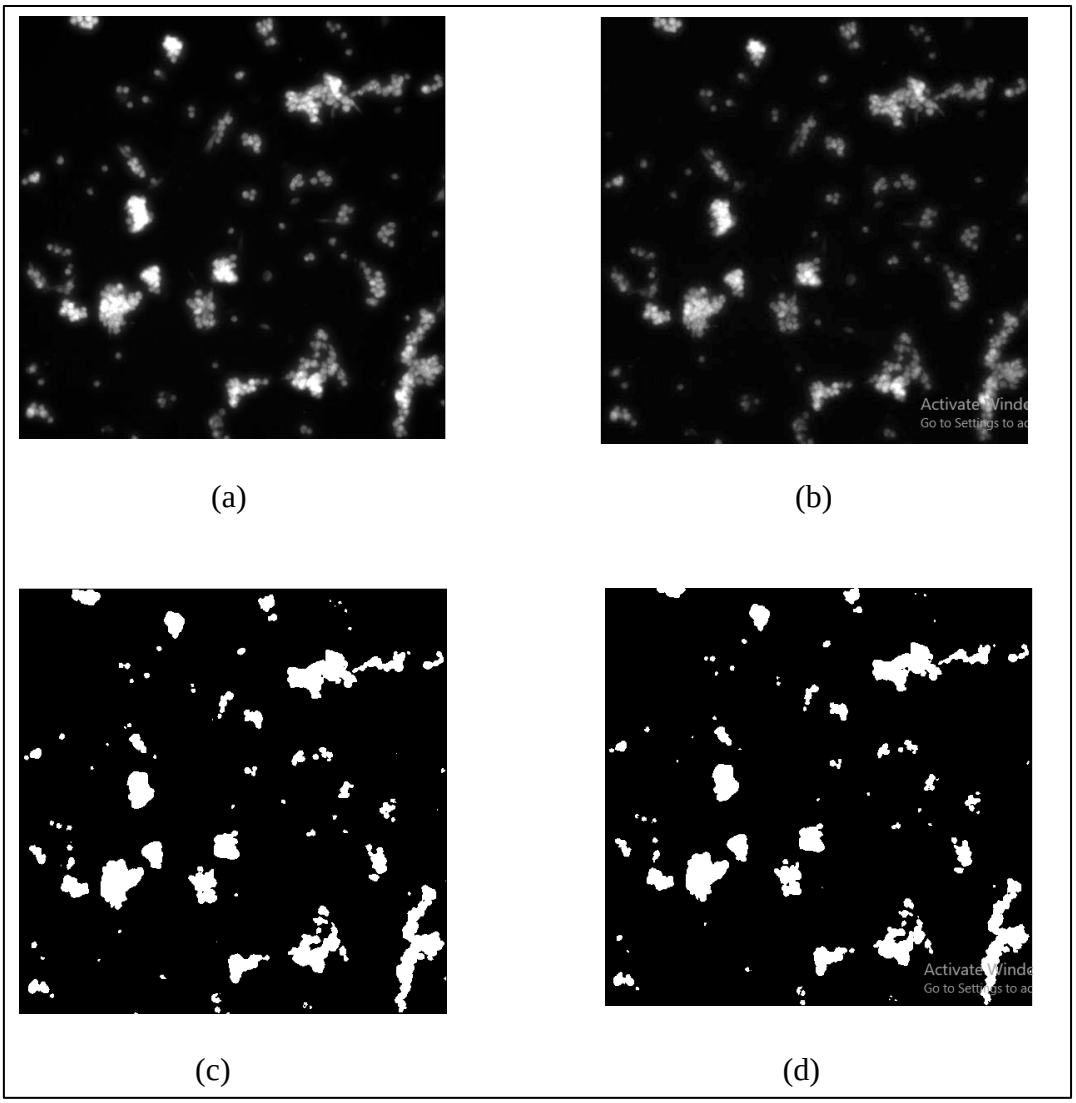

جـامعـــة النجاح الوطنية

كليـــة الدراســـات العليـــا

الطرق التجريبية والنمذجة لدراسة تأثير الإشعاع على مجموعة من الخلايا

إعداد

خلود جرارعة

إشراف

د. أحمد بصلات

د. سامر عبد الله

قدمت هذه الرسالة استكمالا لمتطلبات الحصول على درجة الماجستير في الفيزياء، من كلية الدراسات العليا، في جامعة النجاح الوطنية، نابلس– فلسطين.

2023

الطرق التجريبية والنمذجة لدراسة تأثير الإشعاع على مجموعة من الخلايا

إعداد

خلود جرارعة

إشراف

د. أحمد بصلات

د. سامر عبد الله

الملخص

في السنوات الأخيرة، تم إحراز تطور ملحوظ في فهم السمات المقترحة لعلاج السرطان، ومع ذلك يبقى معدل الإصابة بمرض السرطان عالياً، حتى في القرن الحادي والعشرين لا يزال هناك تحدياً لإيجاد التقنية المثلى لعلاج السرطان. على الرغم من طرق العلاج المعروفة مثل الجراحة، العلاج الكيميائي، العلاج الإشعاعي، العلاج المناعي و العلاج الهرموني، يبقى العلاج الإشعاعي جزءاً مهماً من خطة علاج الورم، الهدف الرئيسي من العلاج الإشعاعي هو التحكم أو تثبيط تكاثر الخلايا السرطانية. بالرغم من هذا كله، إلا أن هناك سمة معروفة للخلايا السرطانية التي تعزز عدوانية الورم وانتشاره الذي يؤدي الى تكهنات سريرية أسوأ، وهذه الصفة تعرف بحمضية بيئة الورم. تأتي هذه الحمضية نتيجة لارتفاع نشاط تحلل السكر للخلايا السرطانية مما يؤدي الى إنتاج كثيف للاكتات. اعتماداً على المعرفة السابقة لخصائص الخلايا السرطانية و فيزياء الإشعاع، سيتم شرح المبادئ والمنهجيات والتقنيات المستخدمة لدراسة تأثير الإشعاع و درجة الحموضة (الداخلية و الخارجية للورم) على نمو خلايا (F98) و هو نوع من الخلايا السرطانية الدبقية المأخوذة من الفئران.

تتكون هذه الدراسة من جزئين، الجزء الاول هو الجزء العملي، حيث تم إجراء العديد من التجارب لدراسة درجة الحموضة الخارجية للورم والتي ممكن أن تكون عامل مهم يؤثر على فعالية العلاج الإشعاعي للسرطان، أولاً، تمت دراسة هذا التأثير على كلاً من نمو الخلايا السرطانية وأيضاً على قدرتها على البقاء على قيد الحياة بعد وضع خلايا (F98) داخل أوساط تختلف في درجة الحموضة وأيضاً استخدام كميات مختلفة

من الإشعاع، توصلت النتائج في هذا الجزء أنه عند تغيير درجة حموضة الوسط سيؤدي إلى تغيير كفاءة تأثير الاشعاع على الخلايا، مما يعطي حجةً لاعتبار درجة الحموضة هدفًا علاجيًا للأبحاث المستقبلية القائمة على جمع العلاج الإشعاعي مع عوامل تنظيم درجة الجموضة. ثانياً، تم حساب درجة الحموضة الداخلية لخلايا (F98) بعد وضع هذه الخلايا داخل أوساط ذات درجات حموضة مختلفة وتعريضها لكميات مختلفة من الإشعاع توصلت نتائج هذه التجربة أنه يمكن اعتبار التغيرات في درجة الحموضة الداخلية للورم بسبب الإشعاع تأثيرًا بيولوجيًا جديدًا للإشعاع على الخلية السرطانية، وكانت هذه النتائج مثيرة للاهتمام للغاية، لكنها لا تزال بحاجة إلى الموافقة عليها. الجزء الثاني من الدراسة كان عبارة عن النمذجة أو المحاكاة الحسابية، حيث تم في هذا العمل بناء نموذج لوصف نمو الخلايا، وكانت نتائج المحاكاة قادرة على إعطاء نفس التغير الذي حصل في البيانات التجريبية. وهناك أيضاً إمكانية تطوير هذه المحاكاة لإضافة المزيد من المتغيرات لإعطاء معلومات أكثر عن النظام.

الكلمات المفتاحية: دبقي، الانتشار، درجة الحموضة، إشعاع، العلاج الإشعاعي.